Co-targeting CDK4/6 and AKT with endocrine therapy prevents progression in CDK4/6 inhibitor and endocrine therapy-resistant breast cancer

Carla L. Alves[1*], Sidse Ehmsen[1,2‡], Mikkel G. Terp[1‡], Neil Portman[3,4], Martina Tuttolomondo[1], Odd L. Gammelgaard[1], Monique F. Hundebøl[1], Kamila Kaminska[5], Lene E. Johansen[1], Martin Bak[6], Gabriella Honeth[5], Ana Bosch[5], Elgene Lim[3,4], Henrik J. Ditzel[1,2,7*]

[1]Department of Cancer and Inflammation Research, Institute of Molecular Medicine, University of Southern Denmark, Odense, Denmark.
[2]Department of Oncology, Institute of Clinical Research, Odense University Hospital, Odense, Denmark.
[3]Garvan Institute of Medical Research, Darlinghurst, Sydney, NSW, Australia.
[4]St. Vincent's Clinical School, Faculty of Medicine, University of New South Wales Sydney, Sydney, NSW, Australia.
[5]Division of Oncology and Pathology, Department of Clinical Sciences, Lund University, Medicon Village, Lund, Sweden.
[6]Department of Pathology, Sydvestjysk Sygehus, Esbjerg, Denmark.
[7]Academy of Geriatric Cancer Research (AgeCare), Odense University Hospital, Odense, Denmark.

[*] Corresponding author: Carla L. Alves, PhD, or Henrik J. Ditzel, MD, PhD, MDSc, Department of Cancer and Inflammation Research, Institute of Molecular Medicine, University of Southern Denmark, J.B. Winsløws Vej 25, 5000 Odense C, Denmark, Tel: +45-65503781, Fax: +45-65503922, calves@health.sdu.dk or hditzel@health.sdu.dk

[‡] These authors contributed equally

Abstract: CDK4/6 inhibitors (CDK4/6i) combined with endocrine therapy have shown impressive efficacy in estrogen receptor-positive advanced breast cancer. However, most patients will eventually progress on this combination, underscoring the need for effective subsequent treatments or better initial therapies. Here, we show that triple inhibition with fulvestrant, CDK4/6i and AKT inhibitor (AKTi) durably impaired growth of breast cancer cells, prevented progression and reduced metastasis of tumor xenografts resistant to CDK4/6i-fulvestrant combination or fulvestrant alone. Importantly, switching from combined fulvestrant and CDK4/6i upon resistance to dual combination with AKTi and fulvestrant did not prevent tumor progression. Furthermore, triple combination with AKTi significantly inhibited growth of patient-derived xenografts resistant to combined CDK4/6i and fulvestrant. Finally, high phospho-AKT levels in metastasis of breast cancer patients treated with a combination of CDK4/6i and endocrine therapy correlated with shorter progression-free survival. Our findings support the clinical development of ER, CDK4/6 and AKT co-targeting strategies following progression on CDK4/6i and endocrine therapy combination, and in tumors exhibiting high phospho-AKT levels, which are associated with worse clinical outcome.

Introduction

Endocrine therapy comprises the most effective targeted therapies for treatment of estrogen receptor-positive (ER+) breast cancer. However, development of resistance to these agents remains a major clinical challenge. The role of cyclin D-CDK4/6 signaling in ER+ breast cancer tumorigenesis and endocrine resistance is well described [1-5]. Importantly, studies have shown that ER+ breast cancer resistant to endocrine therapy is dependent on the cyclin D-CDK4/6 pathway [6,7]. Together, these data supported the clinical investigation of several CDK4/6 inhibitors (CDK4/6i), including palbociclib, ribociclib and abemaciclib, in combination with endocrine therapy. Clinical studies have demonstrated that combined CDK4/6i and endocrine therapy significantly improves progression-free survival (PFS) and overall survival (OS) compared to endocrine therapy alone in ER+ advanced breast cancer, resulting in the approval of CDK4/6i in the first-line setting combined with aromatase inhibitor (AI). Additionally, the combination of CDK4/6i and ER degrader fulvestrant was approved for use following progression on initial AI monotherapy [8-13].

The link between deregulated PI3K/AKT-mTOR pathway and endocrine resistance is also well known [14]. Everolimus, a mTORC1 inhibitor, was shown to prolong PFS in combination with the AI exemestane in ER+ advanced breast cancer after progression on non-steroidal AI [15]. However, inhibition of mTORC1 induces a negative feedback loop that activates AKT, limiting the efficacy of mTORC1 inhibitors [16]. Additionally, alpelisib, an alpha-specific PI3K inhibitor (PI3Ki), has recently been approved for treatment of *PIK3CA*-mutated ER+ advanced breast cancer that progressed on previous endocrine therapy [17]. Notably, it has been suggested that direct blockade of AKT may provide a better treatment option for endocrine-resistant breast cancer, affecting cell survival and ER ligand-independent signaling in both *PIK3CA*-mutant and

wild-type tumors [18]. Currently, there are several AKT inhibitors (AKTi) under clinical investigation, including the pan-AKT kinase catalytic inhibitor capivasertib (AZD5363) that, in combination with fulvestrant, has recently been demonstrated to improve PFS in ER+ metastatic breast cancer patients who progressed on an AI [19]. Interestingly, no difference in response was observed between patients with PI3K/PTEN/AKT pathway activation due to genetic alterations in PI3K/PTEN/AKT and patients without such genetic alterations. A phase III trial is currently evaluating capivasertib in combination with fulvestrant in ER+ metastatic breast cancer patients following progression on an AI (CAPItello-291). Furthermore, a current phase Ib/III trial is evaluating AKTi capivasertib plus palbociclib and fulvestrant versus palbociclib and fulvestrant in ER+ locally advanced, unresectable or metastatic breast cancer (CAPItello-292).

Nonetheless, some patients do not respond to CDK4/6i, and a significant number of patients who initially respond to these drugs will progress, underscoring the need to identify biomarkers and develop more rational drug combinations. Recently, CDK4/6i were found to sensitize *PIK3CA*-mutant tumors to PI3Ki and, conversely, mTORC1/2 inhibitors inhibited growth of CDK4/6i-resistant cells [20,21]. Furthermore, activation of the PI3K/AKT-mTOR pathway has been shown to be a mechanism of early adaptive resistance to CDK4/6i [22]. These data support the use of therapeutic strategies targeting both pathways to prevent the compensatory pathway activation involved in drug resistance. However, combining the available agents targeting the PI3K/AKT-mTOR pathway with the approved CDK4/6i and ER-targeted therapies results in many possible combinations in different lines of therapy, which complicates determining the optimal therapeutic strategy for individual patients. Moreover, overlapping toxicity and high costs further complicate the addition of new targeted agents to standard treatments [23].

Here, we demonstrate that triple combination of the AKTi, CDK4/6i and fulvestrant is required to durably impair growth and prevent progression in ER+ breast cancer cell lines and tumor xenografts resistant to combined therapy with fulvestrant and CDK4/6i or fulvestrant alone. Furthermore, the triple combination significantly inhibited growth of patient-derived xenografts (PDXs) resistant to combined CDK4/6i and fulvestrant. Importantly, switching from fulvestrant and CDK4/6i combination, upon resistance, to the combination of AKTi and fulvestrant did not prevent tumor progression. These data suggest that triple combination with AKTi, CDK4/6i and fulvestrant represents a therapeutic option for tumors that will relapse on standard therapy with fulvestrant alone or in combination with CDK4/6i. Further, we found that high levels of p-AKT in metastatic lesions from ER+ breast cancer patients treated with combination endocrine therapy and CDK4/6i in the advanced setting correlated with shorter PFS. Our findings support the clinical development of triple combinations with fulvestrant, CDK4/6i and AKTi in pre-treated ER+ advanced breast cancer, particularly in tumors exhibiting high levels of p-AKT, to improve patient survival.

Results

Fulvestrant, CDK4/6i and AKTi triple combination therapy is required for durable growth inhibition of fulvestrant-resistant breast cancer cells

We previously demonstrated that cooperation between CDK6 and AKT confers resistance to fulvestrant in ER+ breast cancer cell lines [24]. Furthermore, recent studies have shown that inhibitors of the PI3K/AKT-mTOR pathway synergize with agents targeting the cyclin D/CDK4-6/Rb axis, which supports the use of combinational strategies with inhibitors of both pathways [21,25,26]. However, which therapeutic strategy, endocrine therapy combined with either a

CDK4/6 or a PI3K/AKT-mTOR inhibitor, sequential treatments with these combinations or upfront triple combination, is the best as first-line treatment in endocrine-resistant and -sensitive tumors remains to be defined. Herein, we assessed the efficacy of the AKTi capivasertib, CDK4/6i palbociclib and the ER degrader fulvestrant as single agents and in double and triple combinations in ER+ MCF-7, T47D and ZR-75-1 fulvestrant-resistant and -sensitive breast cancer cell models. The concentrations of CDK4/6i and AKTi used were determined based on the highest IC_{50} between parental and resistant cell lines of each cell model (Supplementary Fig. S1). As expected, fulvestrant alone induced a marked decrease in growth of fulvestrant-sensitive cells (Fig. 1A, 1E and 1I). Although combined fulvestrant and CDK4/6i almost completely inhibited growth of all the fulvestrant-sensitive cell lines and fulvestrant-resistant ZR-75-1 R cells, it had only a limited effect on fulvestrant-resistant 182R-1 (MCF-7 based) and T47D R cells (Fig. 1A-B, 1E-F and 1I-J). Moreover, triple combination with fulvestrant, CDK4/6i and AKTi decreased growth to a greater degree than observed with fulvestrant and CDK4/6i, and was needed to maintain growth inhibition of fulvestrant-resistant 182R-1 and T47D R cells (Fig. 1A-B, 1E-F and 1I-J). In line with these findings, we observed that the triple combination more potently impaired the viability of all cell lines compared to the fulvestrant and CDK4/6i combination (Fig. 1C-D, 1G-H and 1K-L. The efficacy of combined fulvestrant and AKTi was comparable to the approved fulvestrant and CDK4/6i combination (Fig. 1A-L). The additional growth inhibitory effect of the triple combination compared to the standard fulvestrant and CDK4/6i combination was, at least in part, a result of induction of apoptosis (Fig. 2A-C) and cleaved-PARP levels (Fig. 2D). Calculations of the combination index (CI) showed that fulvestrant, CDK4/6i and AKTi exhibited synergistic activity when combined, except for combined fulvestrant and AKTi in ZR-75-1 R cells (Supplementary Fig. S2). Finally, we

examined whether the triple combination could delay the emergence of resistance in a colony outgrowth assay (Fig. 1M-P and Supplementary Fig. S3). We observed that the triple combination suppressed growth of 182R-1 cells up to 8 weeks and T47D R over the entire 12 weeks of treatment (Fig. 1N and 1P), while relatively rapid outgrowth was observed with combined fulvestrant and CDK4/6i or AKTi (1 week for 182R-1 and 3-5 weeks for T47D R). In contrast, no or very slow outgrowth was observed in parental MCF-7 and T47D cells treated with the combination of fulvestrant with either CDK4/6i or AKTi, or the triple combination (Fig. 1M and 1O). ZR-75-1 R cells showed high sensitivity to AKTi and CDK4/6i single agents in the long-term growth assay (Supplementary Fig. S3B). Importantly, the concentration of CDK4/6i used in ZR-75-1 cells based on the IC_{50} value was considerably high (Supplementary Fig. S1A) and palbociclib has been shown to inhibit the proteasomal regulator DYRK1A at 2 μM [27], suggesting an unspecific effect of palbociclib on growth of ZR-75-1 cells. Nevertheless, our data suggest that the approved treatment with fulvestrant combined with a CDK4/6i efficaciously inhibits growth of endocrine-sensitive and some endocrine-resistant breast cancer cells, but simultaneous inhibition of ER, CDK4/6 and AKT is required to durably suppress growth of most of endocrine-resistant cells of different breast cancer models.

Combined targeting of CDK4/6 and AKT efficiently inhibits cyclin D/CDK4-6/Rb and PI3K/AKT-mTOR pathways in ER+ breast cancer cell lines

Next, we evaluated the expression and activation of key molecules of the three cellular signal pathways (ER, cyclin D/CDK4-6/Rb and PI3K/AKT-mTOR) 72 hours after treatment with the targeted inhibitors capivasertib, palbociclib and fulvestrant in MCF-7, T47D and ZR-75-1 breast cancer cell line models (Fig. 2E), as this is when immediate growth suppression induced by palbociclib is released [22]. We observed that the triple combination led to a marked ER decrease

and significantly reduced phosphorylation levels of Rb, PRAS40 and S6 proteins in both fulvestrant-sensitive and -resistant cells (Fig. 2E), indicating inhibition of ER, cyclin D/CDK4-6/Rb and PI3K/AKT-mTOR pathways. Treatment with AKTi induced phosphorylation of AKT, which maintains the protein in a hyperphosphorylated, catalytically inactive state, as previously described [18]. Notably, none of the single agents or combinations without simultaneous targeting of AKT and CDK4/6 produced similarly profound inhibition of the downstream targets of the three pathways compared to the triple combination, particularly in fulvestrant-resistant cells (Fig. 2E). Interestingly, we observed that 182R-1 and ZR-75-1 R fulvestrant-resistant cells exhibited higher levels of phospho-AKT (p-AKT) compared to their corresponding parental cell lines, while T47D R cells showed slightly lower expression of p-AKT compared to parental cells (Fig. 2F). No significant changes were observed in total AKT levels in resistant vs. sensitive cells in the three fulvestrant-resistant cell models (Fig. 2F). Noteworthy, 182R-1 is *PIK3CA* mutant, while ZR-75-1 R is *PIK3CA* wild-type, suggesting that AKT activation is not associated with *PIK3CA* mutation status. Also, MCF-7 cells showed the lowest p-AKT S473 across all models (Fig. 2F) and were treated with the highest dose of AKTi (500nM), while ZR-75-1 and T47D cells exhibited higher p-AKT S473 and were treated with lower doses of AKTi (150 nM and 200 nM, respectively), which suggests that high p-AKT S473 levels correlate with higher AKTi sensitivity, as previously shown [28]. The different expression pattern of p-AKT in T47D/T47D R cells might be associated with its remarkably high expression level in T47D cells compared to the other sensitive cell lines. Nevertheless, these observations suggested that p-AKT could be a potential marker for identification of fulvestrant-resistant tumors that are likely to benefit from treatment with the triple combination.

Co-targeting CDK4/6 and AKT prevents progression of ER+ breast xenografts resistant to fulvestrant

Next, we evaluated the efficacy of fulvestrant, CDK4/6i (50 mg/Kg) and AKTi (100 mg/kg) as monotherapies and in different combinations *in vivo,* using mice bearing 182R-1 tumors. Both CDK4/6i and AKTi were administered orally 5 days a week. Fulvestrant (100 mg/kg) alone, administered subcutaneously once a week, induced tumor regression in MCF-7 xenografts (Fig. 3A and 3C) and, as expected, did not affect the growth of 182R-1 fulvestrant-resistant tumors (Fig. 3B and 3C). Similar results were observed when comparing the end-point tumor weight (Supplementary Fig. S4A and S4B). CDK4/6i as monotherapy reduced tumor growth over a period of 6 weeks, but both double and triple combinations inhibited growth to a greater extent ($p = 0.02$ and $p = 0.01$, respectively) and resulted in tumor regression (Fig. 3D and Supplementary Fig. S4C). Interestingly, hematoxylin and eosin (HE) staining of 182R-1 tumors treated for 6 weeks with vehicle, fulvestrant alone, fulvestrant+CDK4/6i and triple combination with AKTi showed that tumors treated with vehicle or fulvestrant predominantly consisted of vital tumor cells. Tumors treated with combined CDK4/6i and fulvestrant were smaller and contained infiltrating fat cells that were more pronounced in tumors treated with the triple combination wherein only smaller tumor islets containing central degeneration surrounded by fat tissue were observed (Supplementary Fig. S4G). Neither fulvestrant or AKTi monotherapy or combined fulvestrant and AKTi significantly inhibited tumor growth (Supplementary Fig. S4E and S4F). Although the difference between standard combination of fulvestrant and CDK4/6i and triple combination treatment was not significant, a smaller mean of tumor volume and weight was observed for the triple combination group (Fig. 3D and Supplementary Fig. S4C). As the treatment was initiated while the tumors were relatively small (50 mm^3), we next examined

whether the triple combination was more effective than the standard double combination in reducing the volume of tumors allowed to expand to a larger size (250 mm^3) before initiating treatment. Interestingly, significantly greater tumor regression was induced by the triple combination compared to the standard double therapy in these larger tumors at the endpoint, as evaluated by the parametric t-test ($p = 0.01$) and the non-parametric Wilcoxon test ($p = 0.009$, Fig. 3E and Supplementary Fig. S4D). Notably, tumor regression was most prominent during the first 3 weeks of treatment and subsequently stabilized in both the triple and double combination groups (Fig. 3E). Importantly, the triple combination completely blocked tumor regrowth during 8 weeks of treatment, while tumors treated with the standard double combination of fulvestrant and CDK4/6i started to expand after 6 weeks of treatment, suggesting outgrowth of resistant clones (Fig. 3E). We found a statistically significant difference in tumor growth rate between double and triple combinations with linear mixed effects models (GR 7.47, $p = 0.009$, CI 1.88-13.07). Although no significant difference was observed in cleaved caspase-3, we observed decreased expression of the proliferation marker Ki67 in all fulvestrant-resistant tumors treated with triple combination compared to double-combination (Supplementary Fig. S4H), which is in line with our *in vitro* findings (Fig. 1A-D). Furthermore, HE staining showed that tumors treated with the triple combination contained large areas of degeneration and reactive fibrosis (within the indicated circles) surrounded by vital tumor tissue, while only small areas of degeneration and reactive fibrosis were observed in tumors treated with combined CDK4/6i and fulvestrant, and the vital tumor tissue areas were much larger in these tumors (Supplementary Fig. S4H). Together, these findings support the addition of AKTi to the standard combination of fulvestrant and CDK4/6i to maintain inhibition of tumor growth in fulvestrant-resistant tumors.

Combined fulvestrant, CDK4/6i and AKTi is needed to maintain tumor growth inhibition in breast cancer cell lines and tumor xenografts resistant to combined CDK4/6i and fulvestrant

Previous studies have shown that early adaptation to CDK4/6i can be prevented by combination with endocrine therapy, CDK4/6i and a PI3Ki [22]. However, when tumors progress on combined CDK4/6i and endocrine treatment, the question remains as to whether there is a continued benefit of maintaining CDK4/6i and endocrine therapy and adding an inhibitor of PI3K/AKT-mTOR pathway, or whether CDK4/6i should be switched to a PI3K/AKT-mTOR inhibitor. Here, we assessed the efficacy of fulvestrant, CDK4/6i and AKTi as single agents and in different combinations in MCF-7 and T47D breast cancer cell lines exhibiting acquired resistance to combined CDK4/6i and fulvestrant treatment (MPF-R and TPF-R, respectively). These cells were generated by continuous exposure to a high dose of fulvestrant and CDK4/6i over 3-4 months, as detailed in Material and Methods. The concentrations of AKTi used in MPF-R and TPF-R models were similar to those used in MCF-7 and T47D fulvestrant-resistant models and were determined based on the highest IC_{50} between parental and resistant cell lines of each cell model (Supplementary Fig. S1C). We found that growth and viability of the MPF-R and TPF-R cell lines were significantly impaired by the triple combination of fulvestrant, CDK4/6i and AKTi (Fig. 4B, 4D, 4F and 4H). Although combined fulvestrant and AKTi was more effective than the standard combination of fulvestrant and CDK4/6i, it was not sufficient to maintain cell growth inhibition in the resistant cell lines MPF-R and TPF-R (Fig. 4B and 4F). In contrast, fulvestrant combined with either CDK4/6i or AKTi was highly effective in sensitive cells (Fig. 4A, 4C, 4E and 4G). Moreover, we observed that the triple combination inhibited growth of resistant colonies in MPF-R and TPF-R cells over the entire 12 weeks of treatment (Fig. 4I-J).

Together, these data suggest that breast cancer cells resistant to the combination of CDK4/6i and endocrine therapy will rapidly progress on fulvestrant and AKTi, but will benefit from the addition of AKTi to the standard combination of CDK4/6i and fulvestrant. Importantly, we evaluated the efficacy of AKTi when combined with other CDK4/6i's, including ribociclib and abemaciclib, in palbociclib-resistant MPF-R and TPF-R cells (Supplementary Fig. S5) and observed that MPF-R and TPF-R cells exhibited a significantly higher IC50 for the three CDK4/6i compared to M-S and T-S cells, respectively (Supplementary Fig. S5A). The addition of AKTi to the combination of fulvestrant and ribociclib or abemaciclib induced a greater growth inhibition compared to combined CDK4/6i and fulvestrant (Supplementary Fig. S5B-C, respectively). These data suggest that co-targeting CDK4/6 and AKT is efficacious in ER+ breast cancer resistant to the three CDK4/6i's currently clinically approved, which show some differences in the spectrum of target kinases [29]. Furthermore, we observed a marked increase in apoptosis and cleaved-PARP levels in MPF-R cells treated with the triple combination compared to the standard fulvestrant and CDK4/6i combination, although these changes were not observed in TPF-R cells (Fig. 5A-C). We also found that Rb and p-Rb S780 levels were markedly reduced in M-S and T-S cells after treatment with CDK4/6i alone and combined with fulvestrant (Supplementary Fig. S6). Additionally, we observed that treatment with CDK4/6i alone and combined with fulvestrant decreased Rb levels to a lower extent in MPF-R and TPF-R cells than in the parental cells (Supplementary Fig. S6A). p-Rb S780 baseline levels were also significantly lower in MPF-R and TPF-R cells compared to the parental cells (Supplementary Fig. S6B). These data support reduced dependence on the cyclin D1-CDK4/6 pathway in MPF-R and TPF-R cells, as previously shown in other cell line models resistant to CDK4/6i [22]. We observed a marked reduction of p-PRAS40 and p-S6 expression when MPF-R and TPF-R cells were treated

with AKTi (Fig. 5D), consistent with PI3K/AKT-mTOR pathway blockade. Furthermore, MPF-R exhibited higher levels of p-AKT and similar levels of total AKT compared to parental M-S cells, while p-AKT expression was slightly lower and total AKT was higher in TPF-R compared to parental T47D sensitive T-S cells (Fig. 5E).

To further investigate our *in vitro* findings (Fig. 4A-J), we compared the efficacy of the triple and double combinations in MPF-R tumor xenografts. MPF-R cells were orthotopically implanted in the mammary fat pad of mice and, when tumors reached approximately 100 mm^3, treatment with fulvestrant (100 mg/Kg) and CDK4/6i (50 mg/Kg) with or without AKTi (100 mg/Kg) was initiated and continued for 7 weeks. Although the double combination significantly inhibited tumor growth of MPF-R tumors compared to vehicle, it failed to induce tumor regression (Fig. 6A), in contrast with the profound tumor regression observed in 182R-1 fulvestrant-resistant tumors (Fig. 3E). This supports the reduced sensitivity of MPF-R cells to the standard combination of fulvestrant and CDK4/6i. More importantly, the triple combination almost completely inhibited tumor growth over the 7 weeks of treatment, while tumors treated with the double combination started to regrow after 5 weeks (Fig. 6A). Furthermore, a statistically significant difference in tumor size and weight was observed between mice treated with the triple versus double combinations at the endpoint, as evaluated by the parametric t-test and the non-parametric Wilcoxon test (Fig. 6A and Supplementary Fig. S7A). We also found a statistically significant difference in tumor growth rate between double and triple combinations using linear mixed effects models (GR 13.36, $p < 0.0001$, CI 8.41-18.29).

Additionally, we observed a significant change of ER, p-Rb, p-AKT, p-PRAS40 and p-S6 levels in MPF-R tumors treated with the triple combination (Fig. 6B and Supplementary Fig. S7B), similar to our *in vitro* findings (Fig. 5D). Although no significant change in cleaved caspase-3

expression was observed, decreased expression of the proliferation marker Ki67 was found in MPF-R tumors treated with triple combination compared to double combination (Supplementary Fig. S7C-D), which is also in line with our *in vitro* findings (Fig. 4A-D). Furthermore, HE staining showed that tumors treated with combined CDK4/6i and fulvestrant primarily consisted of vital tumor tissue, while tumors treated with the triple combination were smaller and contained larger areas of degeneration and reactive fibrosis (within the indicated circles) or smaller areas of degeneration and lipid infiltration surrounded by vital tumor tissue (Supplementary Fig. S7C).

Next, we evaluated the efficacy of the triple combination with AKTi in a PDX model resistant to combined CDK4/6i and fulvestrant (KCC_P_3837-FPR), generated through continuous exposure of PDX KCC_P_3837 tumors to combined palbociclib and fulvestrant over three passages in mice (Fig. 6C). We observed that PDX KCC_P_3837-FPR mice treated with the triple combination showed a statistically significant ($p = 0.003$) increase in progression-free survival (PFS), with progression defined as tumor width ≥ 5 mm, compared to mice in the combined CDK4/6i and fulvestrant treatment group (Fig. 6D). Decreased Ki67 expression was observed in tumors treated with the triple combination compared to the combined CDK4/6i and fulvestrant (Supplementary Fig. S7D). Furthermore, HE staining showed that PDX tumors treated with the triple combination contained large areas of degeneration and reactive fibrosis (within the indicated circles) surrounded by vital tumor tissue. In contrast, only small areas, if any, of degeneration and reactive fibrosis were observed in tumors treated with combined CDK4/6i and fulvestrant, and the vital tumor tissue area was much larger in these tumors (Supplementary Fig. S7D). Finally, we performed two sets of animal experiments to analyze the effect of the triple combination, combined fulvestrant and CDK4/6i or combined fulvestrant and AKTi in MPF-R

and TPF-R cells using an experimental metastasis model. To mimic the scenario wherein tumor cells under selective pressure of the treatment enter the circulation and subsequently develop metastasis in lungs and liver, we pre-treated the cells *in vitro* for 3 days, which inhibited the signaling pathways without affecting viability, before injection of cells in the tail vein. The triple combination-treated group contained significantly fewer metastasis (defined, approximately, as tumor area > 2500 μm^2) compared to the combined fulvestrant and CDK4/6i-treated group at 6 weeks of treatment in both MPF-R ($p = 0.050$, Fig. 6E) and TPF-R ($p = 0.043$, Fig. 6F) models. For the TPF-R model, the number and size of metastasis was small, likely due to the slow growth rate of these cells (Fig. 6G). Overall, the metastasis was smaller in the triple combination-treated group compared to the fulvestrant and CDK4/6i combination-treated group in both MPF-R ad TPF-R models (Fig. 6G). Furthermore, triple combination-treated group contained significantly fewer metastasis than fulvestrant and AKTi combination-treated group in the MPF-R model ($p = 0.001$) (Fig. 6E and 6G). Together, our findings show that the triple combination of fulvestrant, CDK4/6i and AKTi effectively inhibits growth of tumors that expand on combined fulvestrant and CDK4/6i treatment.

High expression of p-AKT correlates with shorter PFS in ER+ advanced breast cancer treated with combined fulvestrant and CDK4/6i

Next, we investigated the clinical relevance of higher levels of p-AKT in MCF-7 and ZR-75-1 breast cancer cells resistant to fulvestrant (Fig. 2F) and combined fulvestrant and CDK4/6i (MPF-R cells) (Fig. 5E). p-AKT levels in full sections of metastatic lesions of ER+ breast cancer patients treated with endocrine therapy and CDK4/6i in the advanced setting were evaluated by immunohistochemistry. Initially, we determined the cut-off value of p-AKT scoring by evaluating p-AKT levels in a pilot cohort (N = 17), which included patients treated at Odense

University Hospital, Denmark, with a metastatic biopsy obtained in 2019. Although patients included in the pilot cohort had a short clinical follow-up, we determined a cut-off value that showed survival significance in Kaplan-Meier curves (cut-off ≥ 150; $p = 0.03$; Supplementary Fig. S8) and, thus, we selected this value as the cut-off to stratify patients into high and low p-AKT in the validation cohort (N = 84, metastatic biopsy obtained in 2017-2018). Clinical and pathological characteristics of the primary tumor and metastatic disease of patients from both cohorts are shown in Supplementary Table S1 and Table 1, respectively. Although $\chi 2$ and Fisher's exact tests identified a statistically significant difference in primary tumor size between low and high p-AKT groups, this difference was found in both pilot and validation cohorts (Supplementary Table S1). No other differences in clinical and pathological characteristics of primary tumors or metastatic disease were observed in the pilot and validation cohorts (Supplementary Table S1 and Table 1). Kaplan-Meier curves of the validation cohort showed significantly ($p = 0.04$) lower PFS in the high p-AKT group (H-score ≥ 150; 9.87 months) compared with the low p-AKT group (H-score < 150; 15.37 months), corresponding to a 6 month increase in the median time to progression (Fig. 7A). Univariate Cox's proportional hazards regression analysis showed that only p-AKT status was a prognostic factor for PFS for patients treated with combined CDK4/6i and endocrine therapy (HR 2.07, 95% CI of the ratio, 1.00-4.29, $p = 0.049$; Supplementary Table S2). Representative immunohistochemistry stainings of low (Fig. 7B-C) and high (Fig. 7D-E) p-AKT levels are shown. Interestingly, we found that not only patients with *PIK3CA*-mutated tumors exhibited high p-AKT levels and patients with *PIK3CA* wild-type tumor exhibited low p-AKT levels, but the opposite was also observed, suggesting that the level of p-AKT is independent of *PIK3CA* mutation status.

Discussion

CDK4/6i have demonstrated impressive efficacy in combination with an aromatase inhibitor or fulvestrant in ER+ advanced breast cancer. However, not all patients benefit significantly from these combination treatments, and even those who do are expected to eventually progress. Therefore, there is a need to evaluate better and more rational targeted combinations to prevent or overcome resistance to standard CDK4/6i and endocrine therapy combination and identify biomarkers for selection of patients who will benefit from novel targeted combinations. In this study, we show that standard combined CDK4/6i and endocrine therapy does not efficiently suppress growth of ER+ breast cancer cell lines and tumor xenografts resistant to fulvestrant, while the addition of AKTi results in profound growth inhibition. Furthermore, the triple combination of CDK4/6i, AKTi and endocrine therapy efficiently suppressed the growth and reduced metastasis of tumors resistant to standard CDK4/6i and endocrine therapy combinations. This was demonstrated in several orthotopic and experimental metastasis models, as well as in a PDX model resistant to combined CDK4/6i and fulvestrant.

It is well known that growth factor-mediated activation of AKT can regulate ER signaling, resulting in ligand-independent activation of ER genomic pathway [30,31]. Furthermore, high AKT levels have been shown to modulate ER binding and estrogen-regulated gene expression [32]. Activation of AKT has also been associated with resistance to endocrine therapy [33]. Together, these data have led to the clinical development of AKTi in combination with endocrine therapy for ER+ breast cancer. Indeed, the clinical trial FAKTION has recently investigated the addition of AKTi capivasertib to fulvestrant for postmenopausal women with ER+ breast cancer who progressed on an AI, and showed that combined capivasertib and fulvestrant significantly extended PFS compared to fulvestrant monotherapy [19]. However, in our study, we observed that

386 the effect of treatment with fulvestrant combined with AKTi is limited, and resistance quickly
387 develops for MCF-7 and T47D cells resistant to fulvestrant monotherapy. The addition of
388 CDK4/6i was required to suppress growth of resistant clones. Nevertheless, endocrine treatment-
389 sensitive cells showed durable tumor growth inhibition with both fulvestrant plus AKTi or
390 fulvestrant plus CDK4/6i. Although we have only examined the efficacy of a triple combination
391 using fulvestrant as the endocrine agent, it has been previously shown that high levels of AKT
392 activity confer resistance to letrozole and anastrozole [34,35], and thus we believe that triple
393 combination with AKTi, CDK4/6i and AIs might be effective in all AI-resistant tumors.

394 Although the alpha-specific PI3Ki alpelisib has recently showed to significantly improve PFS in
395 *PIK3CA*-mutated ER+ advanced breast cancer that progressed on previous endocrine therapy,
396 this PI3Ki is not active in *PIK3CA* wild-type and *PTEN* null tumors [17]. In contrast, capivasertib
397 has demonstrated efficacy in tumors regardless of *PIK3CA* and *PTEN* status [36]. Indeed, the
398 FAKTION clinical trial showed that the *PIK3CA* mutation did not affect the response to
399 combined capivasertib and fulvestrant in ER+ metastatic breast cancer [19]. These findings concur
400 with the preclinical observations in our study that both *PIK3CA* mutant and *PTEN* wild-type
401 (MCF-7 and T47D) and *PIK3CA* wild-type and *PTEN* null (ZR-75-1) cell lines benefited from
402 the addition of AKTi to the standard combination of fulvestrant and CDK4/6i. Importantly, triple
403 combination of fulvestrant, CDK4/6i and AKTi was required for long-term growth inhibition of
404 our fulvestrant-resistant cells derived from MCF-7 and T47D cell line models (*PIK3CA* mutant).
405 Nevertheless, PI3K controls additional pathways that are independent of AKT, such as the ERK
406 signaling pathway, and therefore AKT blockage might not be able to inhibit tumor growth as
407 efficiently as a specific PI3Ki in all *PIK3CA* mutant tumors [37]. Although significant toxicity was
408 reported in the FAKTION clinical study with combined capivasertib and fulvestrant, particularly

diarrhea, rash, and hyperglycemia, these side effects are also observed with other drugs targeting regulators of PI3K/AKT-mTOR pathway and do not overlap with the palbociclib hematological toxicity profile, indicating that the side effects associated with the addition of CDK4/6i to this double combination might be clinically manageable [19].

Previous studies have suggested that simultaneous blockade of PI3K and CDK4/6 is needed to completely inhibit cyclin D1 [22]. Indeed, upon treatment with CDK4/6i, upregulation of AKT with subsequent accumulation of cyclin D1 and sustained expression of cyclin E2 and CDK2 has been observed, which promotes progression into S-phase contributing to resistance. Initial triple combination of endocrine therapy, CDK4/6i and PI3Ki *in vitro* and in patient-derived xenografts achieved greater cell cycle arrest, decreased cyclin E2 and CDK2 expression with subsequent induction of apoptosis, and induced greater tumor regression than each inhibitor alone [22]. However, this effect was not reproduced in cell lines with acquired resistance to CDK4/6i, suggesting that the combination of CDK4/6i and PI3Ki may more effectively delay resistance in CDK4/6i-naïve tumors [22]. However, preliminary results from the phase II clinical trial (BYLieve) with alpha-selective PI3Ki alpelisib and fulvestrant suggest that this combination may also be efficacious in patients with *PIK3CA* mutations that were previously treated with CDK4/6i, although it is too early for firm conclusions [38]. In line with these findings, we show herein that triple combination with fulvestrant, CDK4/6i and another PI3K/AKT-mTOR inhibitor, AKTi, efficiently suppresses growth of cell lines and reduces tumor progression in cell- and patient-derived xenografts with acquired resistance to CDK4/6i and fulvestrant combination. Interestingly, it has been shown that upregulation of AKT and non-AKT targets of PDK1 lead to aberrant cell-cycle progression in ribociclib-resistant cell lines [26]. Additionally, it has been recently found that *PTEN*-deficient cells exhibit cross-resistance to CDK4/6i and alpha-selective

PI3Ki, mediated by AKT activation, which can be overcome by treatment with AKTi [39]. It is noteworthy that in this study, some CDK4/6i-resistant tumors retained *PTEN,* indicating that other mechanisms also mediate resistance to CDK4/6i [39]. Nevertheless, the data presented in our study showed that *PTEN* wild-type cell lines and tumor xenografts resistant to CDK4/6i and fulvestrant (MPF-R and TPF-R cells) benefited from AKT inhibition, demonstrating the need for clinical trials of AKTi in combination with standard CDK4/6i and endocrine therapy in the post CDK4/6i-setting independent of the tumor *PTEN* status. A phase Ib/III trial has recently begun to evaluate the AKTi capivasertib plus palbociclib and fulvestrant versus palbociclib and fulvestrant in ER+ locally advanced, unresectable or metastatic breast cancer (CAPItello-292), further supporting the clinical relevance of our study.

Furthermore, we observed in this study that MCF-7 and ZR-75-1 breast cancer cell lines resistant to endocrine therapy exhibited higher levels of p-AKT compared to sensitive cells, in line with previous findings of a significant increase in p-AKT and high AKT kinase activity in antiestrogen-resistant cell lines [40]. In addition, it has previously been shown that breast cancer patients with p-AKT-positive tumors correlated with worse clinical outcome on endocrine therapy compared to patients with p-AKT-negative tumors [41]. Importantly, our MCF-7-derived breast cancer cell line resistant to the combination of fulvestrant and CDK4/6i also expressed higher p-AKT levels compared to the respective parental cell line. Indeed, activation of the PI3K/AKT-mTOR pathway by PDK1-mediated phosphorylation of AKT (S477/T479) in ribociclib□resistant breast cancer cells has been previously shown [26]. However, the role of p-AKT as a prognostic or predictive biomarker in CDK4/6i-treated patients has not been investigated. Although many biomarkers of resistance to CDK4/6i have been evaluated in preclinical and clinical studies, including Rb loss or mutation, p16 loss, *PIK3CA* mutation, *FAT1*

mutation, aberrant FGFR pathway, CDK6, cyclin D1 and cyclin E amplification, and other D-cyclin-activating features, biomarkers with clinical validity have yet to be identified and represent an unmet need [42-48]. Here, we demonstrated the prognostic value of p-AKT levels in advanced ER+ breast cancer patients treated with CDK4/6i and endocrine therapy. Based on our findings, we suggest that patients with metastasis exhibiting high levels of p-AKT are associated with worse prognosis on treatment with standard CDK4/6i and endocrine therapy and may benefit from the addition of an AKTi to improve survival.

Methods

Cell lines and anti-tumor agents

The original MCF-7 and T47D cell lines were obtained from the Breast Cancer Task Force Cell Culture Bank, Mason Research Institute and the original ZR-75-1 cell line was obtained from the American Type Culture Collection (ATCC). Development of fulvestrant-resistant cell line 182R-1 from MCF-7/S0.5 cells (designated as MCF-7 throughout the manuscript) has been previously described [49]. MCF-7 cells were routinely propagated in phenol red-free Dulbecco's Modified Eagle Medium DMEM/F12 (Gibco) supplemented with 1% glutamine (Gibco), 1% heat-inactivated fetal bovine serum (FBS; Sigma-Aldrich) and 6 ng/ml insulin (Sigma-Aldrich). 182R-1 cells were maintained in the same growth medium as MCF-7 cells supplemented with 100 nM fulvestrant. MCF-7-derived cell lines resistant to combined CDK4/6i and fulvestrant (MPF-R) were developed from 182R-1 cells by prolonged treatment (4 months) with 150-200 nM of CDK4/6i and 100 nM of fulvestrant and maintained in the same growth medium as 182R-1 cells supplemented with 200 nM CDK4/6i. MCF-7-sensitive cells grown in parallel with MPF-R cells were designated M-S. T47D cells were maintained in RPMI 1640 media without phenol

red supplemented with 1% glutamine, 5% FBS and 8 µg/ml insulin. Development of T47D-derived fulvestrant-resistant cell lines (T47D R) has been previously described [50]. T47D cells resistant to fulvestrant and CDK4/6i (TPF-R) were established from T47D R cells by long-term treatment (3 months) with 100 nM fulvestrant and 150-200 nM CDK4/6i and maintained in the same growth medium as T47D R cells supplemented with 200 nM CDK4/6i. T47D-sensitive cells grown in parallel with TPF-R were designated T-S. ZR-75-1 cells were routinely propagated in Roswell Park Memorial Institute (RPMI) 1640 medium (Gibco) supplemented with 10% FBS, 1% HEPES (Gibco) and 1% Penicillin/Streptomycin (Gibco). ZR-75-1 cells were used to establish the fulvestrant-resistant cell line ZR-75-1 R by long-term (8 weeks) exposure to increasing concentrations of fulvestrant from 100 pM to a final concentration of 100 nM. ZR-75-1 R cells were grown in the same growth media as the parental cell line supplemented with 100 nM fulvestrant. Cells were grown in a humidified atmosphere of 5% CO_2 at 37°C. All cell lines underwent DNA authentication using Cell ID™ System (Promega) and mycoplasma testing (Lonza) before the described experiments. Fulvestrant (ICI 182,780, Tocris) was dissolved in ethanol 96%, AKTi capivasertib (HY-15431, MedchemExpress), CDK4/6i ribociclib succinate hydrate (HY-15777C, MedchemExpress) and CDK4/6i abemaciclib (HY-16297A, MedchemExpress) were dissolved in DMSO (Sigma-Aldrich) and CDK4/6i palbociclib isothiocyanate (HY-A0065, MedchemExpress) was dissolved in water. The concentrations of CDK4/6i and AKTi to be used for *in vitro* experiments were determined based on the IC_{50} for each cell line model.

Western blotting

Whole cell extracts were obtained using RIPA buffer (50 mM Tris HCl (pH 8), 150 mM NaCl (pH 8), 1% IgePAL 630, 0.5% sodium deoxycholate, 0.1% SDS) containing protease and

phosphatase inhibitors Complete and PhosSTOP (Roche). The protein concentration of the lysate samples was determined using Pierce BCA Protein Assay Kit (Thermo Fisher Scientific) and the optical density (OD) was measured at 562 nm in the microplate reader Paradigm (Beckman Coulter). 5-30 μg of total protein lysate was loaded on a 4-20% SDS-PAGE gel (Bio-Rad) under reducing conditions and electroblotted onto a PVDF transfer membrane (Bio-Rad). Membranes were blocked in Tris-buffered saline (TBS), 0.1% Tween-20 (Sigma-Aldrich) containing 5% non-fat dry milk powder (Sigma-Aldrich) for one hour at room temperature. The following primary antibodies were used according to the manufacturer´s protocol: anti-ER (RM-9101-S1) from Thermo Fisher Scientific; anti-p-Rb S780 (3590), anti-Rb (9309), anti-p-AKT S473 (4060), anti-AKT (pan) (4685), anti-p-PRAS40 T246 (2997), anti-PRAS40 (2691), anti-p-S6 S235/236 (2211), anti-S6 (2217), anti-cleaved PARP (9541), anti-PARP (9532), anti-Xiap (2042), anti-Bcl-xl (2762), anti-Bax (2772) from Cell Signaling; and anti-GAPDH (sc-32233) from Santa Cruz Biotechnology as loading control. Secondary antibodies horseradish peroxidase (HRP)-conjugated goat anti-mouse (#P0447, Dako) and HRP-conjugated goat anti-rabbit (#P0448, Dako) were incubated in blocking buffer for one hour at room temperature. Membranes were developed with Clarity™ Western ECL Substrate (Bio-Rad) and visualized on Fusion-Fx7-7026 WL/26MX instrument (Vilbaer).

Cell growth, viability and apoptosis assays

Cells were seeded at 750-4000 cells/well in 96-well plates and allowed to attach for 24 hours before drugs or vehicle were added. Evaluation of cell growth was performed using crystal violet-based colorimetric assay [51] and the OD was analyzed at 570 nm in Paradigm reader. Cell viability was evaluated by CellTiter-Blue (Promega) according to the manufacturer´s instructions and fluorescence was measured at 560/590 nm in Paradigm reader. Apoptosis was assessed using

524 the Cell Death Detection ELISA^{Plus} kit (Roche) according to the manufacturer's instructions and
525 the OD was analyzed at 405/490 nm in Paradigm reader. Colony outgrowth assay was performed
526 as previously described [52].

527 **Drug interaction analysis**

528 Cells were seeded at 2500 cells/well and allowed to attach for 24 hours before drugs or vehicle
529 were added. Cells were treated with increasing doses of palbociclib, capivasertib, and fulvestrant
530 or an equipotent combination of the inhibitors and incubated at 5% CO_2 and 37°C for 3 days.
531 Cell growth was evaluated using crystal violet-based colorimetric assay and interactions were
532 calculated with Compusyn software (ComboSyn, Inc.), based on the combination index (CI)
533 equation from Chou-Talalay method [53]. Drug interaction was scored as follows: CI = 1 is
534 additive, CI < 1 is synergistic, CI > 1 is antagonistic.

535 **Xenograft studies**

536 For primary tumor growth, MCF-7, 182R-1 and MPF-R cells were harvested using trypsin
537 (Sigma-Aldrich) and 1 x 10^6 cells were resuspended in 50 ul of extracellular matrix (ECM) from
538 Engelbreth-Holm-Swarm sarcoma (Sigma-Aldrich) and injected orthotopically into the
539 mammary fat pad of 7-week-old female NOG CIEA mice (Taconic) without exogenous estrogen
540 supplements. When tumors reached a certain size (indicated in the figure legend), mice were
541 weighted and randomized into treatment groups. For the experimental metastasis model, MPF-R
542 and TPF-R were harvested using trypsin and 1 x 10^6-2 x 10^6 cells were resuspended in 100-400
543 ul of culture media. 1 x 10^6 cells were inoculated into the lateral tail vein of 7-week-old female
544 NOG CIEA mice. Fulvestrant (Faslodex, AstraZeneca) was formulated at 20 mg/ml in castor oil
545 (Sigma-Aldrich) and administrated once a week subcutaneously. Capivasertib and palbociclib,
546 both from MedchemExpress, were formulated at 20 and 10 mg/ml, respectively, in 25% w/v

HPB cyclodextrin (Sigma-Aldrich) with sonication and administered 5 days a week by oral gavage. Treatment was continued for 5-8 weeks. For the orthotopic model tumor volume was calculated as: tumor volume = 0.5 x (length) x $(width)^2$. For the experimental metastasis model, visualization and quantification of metastasis in the lungs at the endpoint were performed by immunohistochemistry using anti-cytokeratin antibody on full lung sections from 3 different depths. Slides were scanned and analyzed using ndp.view 2.3.14 software (Hamamatsu). The amount of metastasis (defined, approximately, as > 2500 μm^2) relative to lung area was subsequently determined by ImageJ analysis as previously described [54] in a blinded setup. A similar approach was used to quantify the metastatic burden for the TPF-R model, but because the metastasis were quite small in this model, metastasis was measured manually in a blinded setup. All animal experiments were approved by the Experimental Animal Committee of The Danish Ministry of Justice and were performed at the animal core facility at University of Southern Denmark. Mice were housed under pathogen-free conditions with *ad libitum* food and water.

PDX model

KCC_P_3837 was derived from an untreated grade 3, ER+, PR+, HER2- primary invasive ductal carcinoma. KCC_P_3837-FPR (resistant to combined CDK4/6i and fulvestrant) was generated through continuous exposure of KCC_P_3837 tumors to the combination of palbociclib (50 mg/kg in water, 5 days per week by oral gavage) and fulvestrant (5 mg/kg in peanut oil, once weekly via sub-cutaneous injection) over several passages in mice. At each passage, tumors were established to a width of 5 mm before treatment commenced. The parental PDX was responsive to treatment with fulvestrant and palbociclib alone and in combination. A fresh KCC_P_3837-FPR PDX constituting the third passage subjected to selection was harvested and 4 mm^3 sections

were implanted into the 4th inguinal mammary gland of 6–8-week-old female NOD-SCID-IL2γR−/− mice (Australian BioResources Pty Ltd). After two weeks to allow for recovery from surgery, mice were randomized to two treatment arms: combined fulvestrant (100 mg/kg in castor oil, once weekly via sub-cutaneous injection) and palbociclib (25 mg/kg in 2.5% DMSO, 25% β-cyclodextrin, 5 days per week by oral gavage); and triple combination of fulvestrant, palbociclib and capivasertib (100 mg/kg in 2.5% DMSO, 25% β-cyclodextrin, 5 days per week by oral gavage). Tumor growth was supported by implantation of a silastic pellet containing 0.36 mg 17β-estradiol and was monitored visually and by caliper measurement. Endpoint events were tumor width of at least 5 mm (defined as progression) or 60 days of treatment. Procedures and endpoints involving laboratory animals were approved by the Garvan Institute of Medical Research Animal Ethics Committee (protocols 15/25, 18/20 and 18/26).

Clinical samples and endpoints

FFPE metastatic lesions from ER+ breast cancer patients treated with combined CDK4/6i and endocrine therapy in the advanced setting were selected retrospectively by database extraction from the archives of the Department of Pathology at Odense University Hospital (OUH) (N = 115). The inclusion criteria were ER+ breast cancer patients treated with combined CDK4/6i and endocrine therapy in the advanced setting who had undergone surgery or biopsy for advanced stage disease at OUH, and for whom complete clinical information and pathological verification that the metastatic lesion was of breast cancer origin was available. Exclusion criteria were insufficient tumor material in the FFPE block and metastatic biopsy only available after commencing treatment with combined CDK4/6i and endocrine therapy. These parameters yielded N = 101 patients. Patients with metastatic biopsies from 2019 (N = 17) were included in a pilot cohort that was used to select the cut-off based on the survival significance. Patients with

metastatic biopsies obtained before 2019 (N = 84) were included in the validation cohort and the cut-off selected in the pilot cohort was applied to stratify patients into p-AKT low and high groups. Tumors were defined ER+ if ≥ 1% of the tumor cells were stained positive. Progression-free survival (PFS) was defined as the time from initiation of combined endocrine therapy and CDK4/6i treatment until disease progression or death. All clinical samples were coded to maintain patient confidentiality and studies were approved by the Ethics Committee of the Region of Southern Denmark and Copenhagen and Frederiksberg Counties (approval no S-2008-0115).

Immunohistochemistry

FFPE sections (4 μm) of mice tumors and lungs and patients' metastatic lesions were cut with a microtome, mounted on ChemMateTM Capillary Gap Slides (Dako), dried at 60 °C, deparaffinized, and hydrated. Endogenous peroxidase was blocked by 1.5% hydrogen peroxide in TBS buffer, pH 7.4, for 10 min. Antigen retrieval was performed by pretreatment with cell conditioner 1 (CC1) buffer for 32 minutes at 100°C or 36 minutes at 36°C, or by boiling sections in T-EG solution/TRS buffer (Dako). Primary antibodies used were: anti-Ki67 (790-4286) antibody from Ventana Medical Systems, anti-cleaved caspase-3 antibody (9664) from Cell Signaling Technology, anti-cytokeratin antibody (M351501-2) from Agilent and anti-pAKT S473 (4060) antibody from Cell Signaling Technology. Primary antibody binding was detected with Optiview-DAB (8-8) for anti-Ki67 and anti-cytokeratin, EnV, FLEX/HRP+ Rabbit LINK 15-30 for anti-cleaved caspase-3 and DAB detection kit (Ventana Medical Systems) for anti-pAKT. Sections were also stained with hematoxylin and eosin (HE). Microscopy was performed on a Leica DMLB microscope (200x/numerical aperture (NA) 1.25, Leica Microsystems) using LasV3.6 acquisition software. The Ki67 and cleaved caspase-3 staining was quantified by

scanning a representative area of the tumors in each treatment group using ImageJ analysis, as previously described [54]. Evaluation of the clinical samples was performed by an experienced breast pathologist in a blinded setup. p-AKT expression was observed in cell nucleus and cytoplasm and tumors were scored based on the H-score calculated by multiplying the percentage of positive tumor cells (0%-100%) by the staining intensity (0-3). The cut-off value for high (H-score ≥ 150) vs. low (H-score < 150) was determined in the pilot cohort based on the survival significance, and the same cut-off was then applied to the validation cohort.

Statistical Analysis

A two-tailed t-test, ANOVA or Mann-Whitney-Wilcoxon test were employed for *in vitro* and *in vivo* studies (indicated in the figure legend). Grubbs's test was used to find and exclude a single outlier in the dataset. Analysis of growth rate of mice tumors between different treatment groups was performed by linear mixed effects model with categorical treatment groups and continuous time as fixed effects including the interaction. The linear mixed effects model contains a random effect for the individual tumors to consider repeated measurements within each mouse. The group specific time slope is referred to as growth rates (GR). For the PDX model, event curves were calculated using the in-built survival analysis, and curves were compared using the log-rank test. For the clinical data, survival curves were generated by Kaplan-Meier estimates by log-rank test to estimate the correlation between p-AKT expression and PFS. Association between p-AKT expression and patient clinicopathological parameters was determined by Fisher's exact and chi-square (χ^2) tests. Cox proportional hazard regression model was used to assess the adjusted hazard ratio (HR) of PFS by p-AKT expression and clinicopathological characteristics. For statistical analysis, STATA v16.0 (STATACorp) and GraphPad Pism v8 (GraphPad Software, Inc.) were used. p values < 0.05 were considered statistically significant.

Acknowledgements: We would like to thank Anne E. Lykkesfeldt for providing MCF-7 and T47D fulvestrant-resistant cell line models, Lisbet Mortensen and Ole Nielsen at the Department of Pathology, Odense University Hospital, for excellent technical assistance with the immunohistochemistry, and M. Kat Occhipinti for editorial assistance.

Author Contributions: Conceptualization, C.L.A. and H.J.D.; Methodology, C.L.A., S.E., M.G.T., N. P., M.T., O. L. G., K. K., L.E.J., G.H., A.B., E. L. and H.J.D.; Investigation, C.L.A., S.E., M.G.T., N. P., M.T., O. L. G., M.F.H., L.E.J and M.B.; Writing – Original Draft, C.L.A. and H.J.D.; Writing – Review & Editing, all authors; Funding Acquisition, C.L.A. and H.J.D.; Resources, H.J.D.; Supervision, H.J.D.

Competing Interests: The authors declare no competing interests.

Data availability: The authors declare that the data supporting the findings of this study are available within the paper and its supplementary information files.

References

1. Bosco, E. E. et al., The retinoblastoma tumor suppressor modifies the therapeutic response of breast cancer. *J. Clin. Invest.* **117**, 218-228 (2007).
2. Rudas, M. et al., Cyclin D1 expression in breast cancer patients receiving adjuvant tamoxifen-based therapy. *Clin. Cancer Res.* **14**, 1767-1774 (2008).
3. Lange, C. A., Yee, D., Killing the second messenger: targeting loss of cell cycle control in endocrine-resistant breast cancer. *Endocr. Relat. Cancer* **18**, C19-24 (2011).
4. Thangavel, C. et al., Therapeutically activating RB: reestablishing cell cycle control in endocrine therapy-resistant breast cancer. *Endocr. Relat. Cancer* **18**, 333-345 (2011).
5. Cancer Genome Atlas, N., Comprehensive molecular portraits of human breast tumours. *Nature* **490**, 61-70 (2012).
6. Finn, R. S. et al., PD 0332991, a selective cyclin D kinase 4/6 inhibitor, preferentially inhibits proliferation of luminal estrogen receptor-positive human breast cancer cell lines in vitro. *Breast Cancer Res.* **11**, R77 (2009).
7. Miller, T. W. et al., ERalpha-dependent E2F transcription can mediate resistance to estrogen deprivation in human breast cancer. *Cancer Discov.* **1**, 338-351 (2011).

8. Turner, N. C. et al., Palbociclib in Hormone-Receptor-Positive Advanced Breast Cancer. *N. Engl. J. Med.* **373**, 209-219 (2015).
9. Finn, R. S. et al., Palbociclib and Letrozole in Advanced Breast Cancer. *N. Engl. J. Med.* **375**, 1925-1936 (2016).
10. Hortobagyi, G. N. et al., Ribociclib as First-Line Therapy for HR-Positive, Advanced Breast Cancer. *N. Engl. J. Med.* **375**, 1738-1748 (2016).
11. Sledge, G. W., Jr. et al., MONARCH 2: Abemaciclib in Combination With Fulvestrant in Women With HR+/HER2- Advanced Breast Cancer Who Had Progressed While Receiving Endocrine Therapy. *J. Clin. Oncol.* **35**, 2875-2884 (2017).
12. Goetz, M. P. et al., MONARCH 3: Abemaciclib As Initial Therapy for Advanced Breast Cancer. *J. Clin. Oncol.* **35**, 3638-3646 (2017).
13. Im, S. A. et al., Overall Survival with Ribociclib plus Endocrine Therapy in Breast Cancer. *N. Engl. J. Med.* **381**, 307-316 (2019).
14. Miller, T. W. et al., Hyperactivation of phosphatidylinositol-3 kinase promotes escape from hormone dependence in estrogen receptor-positive human breast cancer. *J. Clin. Invest.* **120**, 2406-2413 (2010).
15. Baselga, J. et al., Everolimus in postmenopausal hormone-receptor-positive advanced breast cancer. *N. Engl. J. Med.* **366**, 520-529 (2012).
16. O'Reilly, K. E. et al., mTOR inhibition induces upstream receptor tyrosine kinase signaling and activates Akt. *Cancer Res.* **66**, 1500-1508 (2006).
17. André, F. et al., Alpelisib for PIK3CA-Mutated, Hormone Receptor–Positive Advanced Breast Cancer. *N. Engl. J. Med.* **380**, 1929-1940 (2019).
18. Ribas, R. et al., AKT Antagonist AZD5363 Influences Estrogen Receptor Function in Endocrine-Resistant Breast Cancer and Synergizes with Fulvestrant (ICI182780) In Vivo. *Mol. Cancer Ther.* **14**, 2035-2048 (2015).
19. Jones, R. H. et al., Capivasertib (AZD5363) plus fulvestrant versus placebo plus fulvestrant after relapse or progression on an aromatase inhibitor in metastatic ER-positive breast cancer (FAKTION): A randomized, double-blind, placebo-controlled, phase II trial. *J. Clin. Oncol.* **37**, 1005-1005 (2019).
20. Vora, S. R. et al., CDK 4/6 inhibitors sensitize PIK3CA mutant breast cancer to PI3K inhibitors. *Cancer Cell* **26**, 136-149 (2014).
21. Michaloglou, C. et al., Combined Inhibition of mTOR and CDK4/6 Is Required for Optimal Blockade of E2F Function and Long-term Growth Inhibition in Estrogen Receptor-positive Breast Cancer. *Mol. Cancer Ther.* **17**, 908-920 (2018).
22. Herrera-Abreu, M. T. et al., Early Adaptation and Acquired Resistance to CDK4/6 Inhibition in Estrogen Receptor-Positive Breast Cancer. *Cancer Res.* **76**, 2301-2313 (2016).
23. Portman, N. et al., Overcoming CDK4/6 inhibitor resistance in ER positive breast cancer. *Endocr. Relat. Cancer* (2018).
24. Alves, C. L. et al., High CDK6 Protects Cells from Fulvestrant-Mediated Apoptosis and is a Predictor of Resistance to Fulvestrant in Estrogen Receptor-Positive Metastatic Breast Cancer. *Clin. Cancer Res.* **22**, 5514-5526 (2016).
25. Goel, S. et al., Overcoming Therapeutic Resistance in HER2-Positive Breast Cancers with CDK4/6 Inhibitors. *Cancer Cell* **29**, 255-269 (2016).
26. Jansen, V. M. et al., Kinome-Wide RNA Interference Screen Reveals a Role for PDK1 in Acquired Resistance to CDK4/6 Inhibition in ER-Positive Breast Cancer. *Cancer Res.* **77**, 2488-2499 (2017).

27. Fry, D. W. et al., Specific inhibition of cyclin-dependent kinase 4/6 by PD 0332991 and associated antitumor activity in human tumor xenografts. *Mol. Cancer Ther.* **3**, 1427-1438 (2004).
28. Gris-Oliver, A. et al., Genetic Alterations in the PI3K/AKT Pathway and Baseline AKT Activity Define AKT Inhibitor Sensitivity in Breast Cancer Patient-derived Xenografts. *Clin. Cancer Res.* **26**, 3720-3731 (2020).
29. Hafner, M. et al., Multiomics Profiling Establishes the Polypharmacology of FDA-Approved CDK4/6 Inhibitors and the Potential for Differential Clinical Activity. *Cell. Chem. Biol.* **26**, 1067-1080 e1068 (2019).
30. Kato, S. et al., Activation of the estrogen receptor through phosphorylation by mitogen-activated protein kinase. *Science* **270**, 1491-1494 (1995).
31. Sun, M. et al., Phosphatidylinositol-3-OH Kinase (PI3K)/AKT2, activated in breast cancer, regulates and is induced by estrogen receptor alpha (ERalpha) via interaction between ERalpha and PI3K. *Cancer Res.* **61**, 5985-5991 (2001).
32. Bhat-Nakshatri, P. et al., AKT alters genome-wide estrogen receptor alpha binding and impacts estrogen signaling in breast cancer. *Mol. Cell. Biol.* **28**, 7487-7503 (2008).
33. Tokunaga, E. et al., Activation of PI3K/Akt signaling and hormone resistance in breast cancer. *Breast Cancer* **13**, 137-144 (2006).
34. Beeram, M. et al., Akt-induced endocrine therapy resistance is reversed by inhibition of mTOR signaling. *Ann. Oncol.* **18**, 1323-1328 (2007).
35. Rechoum, Y. et al., AR collaborates with ERalpha in aromatase inhibitor-resistant breast cancer. *Breast Cancer Res. Treat.* **147**, 473-485 (2014).
36. Dienstmann, R., Rodon, J., Serra, V., Tabernero, J., Picking the Point of Inhibition: A Comparative Review of PI3K/AKT/mTOR Pathway Inhibitors. *Mol. Cancer Ther.* **13**, 1021-1031 (2014).
37. Costa, C., Bosch, A., The Strategy of PIKing a Target: What Is AKTually Most Effective? *Clin. Cancer Res.* **24**, 2029-2031 (2018).
38. Rugo, H. S. et al., Alpelisib (ALP) + endocrine therapy (ET) in patients (pts) with PIK3CA-mutated hormone receptor-positive (HR+), human epidermal growth factor-2-negative (HER2-) advanced breast cancer (ABC): First interim BYLieve study results. *J. Clin. Oncol.* **37**, 1040-1040 (2019).
39. Costa, C. et al., PTEN loss mediates clinical cross-resistance to CDK4/6 and PI3Kalpha inhibitors in breast cancer. *Cancer Discov.* **10**, 72-85 (2020).
40. Frogne, T. et al., Antiestrogen-resistant human breast cancer cells require activated protein kinase B/Akt for growth. *Endocr. Relat. Cancer* **12**, 599-614 (2005).
41. Tokunaga, E. et al., The association between Akt activation and resistance to hormone therapy in metastatic breast cancer. *Eur. J. Cancer* **42**, 629-635 (2006).
42. Finn, R. S. et al., The cyclin-dependent kinase 4/6 inhibitor palbociclib in combination with letrozole versus letrozole alone as first-line treatment of oestrogen receptor-positive, HER2-negative, advanced breast cancer (PALOMA-1/TRIO-18): a randomised phase 2 study. *Lancet Oncol.* **16**, 25-35 (2015).
43. O'Leary, B. et al., The Genetic Landscape and Clonal Evolution of Breast Cancer Resistance to Palbociclib plus Fulvestrant in the PALOMA-3 Trial. *Cancer Discov.* **8**, 1390-1403 (2018).
44. Condorelli, R. et al., Polyclonal RB1 mutations and acquired resistance to CDK 4/6 inhibitors in patients with metastatic breast cancer. *Ann. Oncol.* **29**, 640-645 (2018).

45. Li, Z. et al., Loss of the FAT1 Tumor Suppressor Promotes Resistance to CDK4/6 Inhibitors via the Hippo Pathway. *Cancer Cell* **34**, 893-905 e898 (2018).
46. Turner, N. C. et al., Cyclin E1 Expression and Palbociclib Efficacy in Previously Treated Hormone Receptor-Positive Metastatic Breast Cancer. *J. Clin. Oncol.* **37**, 1169-1178 (2019).
47. Finn, R. S. et al., Biomarker Analyses of Response to Cyclin Dependent Kinase 4/6 Inhibition and Endocrine Therapy in Women With Treatment-Naïve Metastatic Breast Cancer. *Clin. Cancer Res.* **26**, 110-121 (2020).
48. Formisano, L. et al., Aberrant FGFR signaling mediates resistance to CDK4/6 inhibitors in ER+ breast cancer. *Nat. Commun.* **10**, 1373 (2019).
49. Lykkesfeldt, A. E., Larsen, S. S., Briand, P., Human breast cancer cell lines resistant to pure anti-estrogens are sensitive to tamoxifen treatment. *Int. J. Cancer* **61**, 529-534 (1995).
50. Kirkegaard, T. et al., T47D breast cancer cells switch from ER/HER to HER/c-Src signaling upon acquiring resistance to the antiestrogen fulvestrant. *Cancer Lett.* **344**, 90-100 (2014).
51. Lundholt, B. K., Briand, P., Lykkesfeldt, A. E., Growth inhibition and growth stimulation by estradiol of estrogen receptor transfected human breast epithelial cell lines involve different pathways. *Breast Cancer Res. Treat.* **67**, 199-214 (2001).
52. Tricker, E. M. et al., Combined EGFR/MEK Inhibition Prevents the Emergence of Resistance in EGFR-Mutant Lung Cancer. *Cancer Discov.* **5**, 960-971 (2015).
53. Chou, T. C., Talalay, P., Quantitative analysis of dose-effect relationships: the combined effects of multiple drugs or enzyme inhibitors. *Adv. Enzyme Regul.* **22**, 27-55 (1984).
54.OpenWetWare. Sean Lauber:ImageJ - Threshold analysis 2012, https://openwetware.org/mediawiki/index.php?title=Sean_Lauber:ImageJ_-_Threshold_Analysis&oldid=595746.

Figures and Figure legends

Figure 1

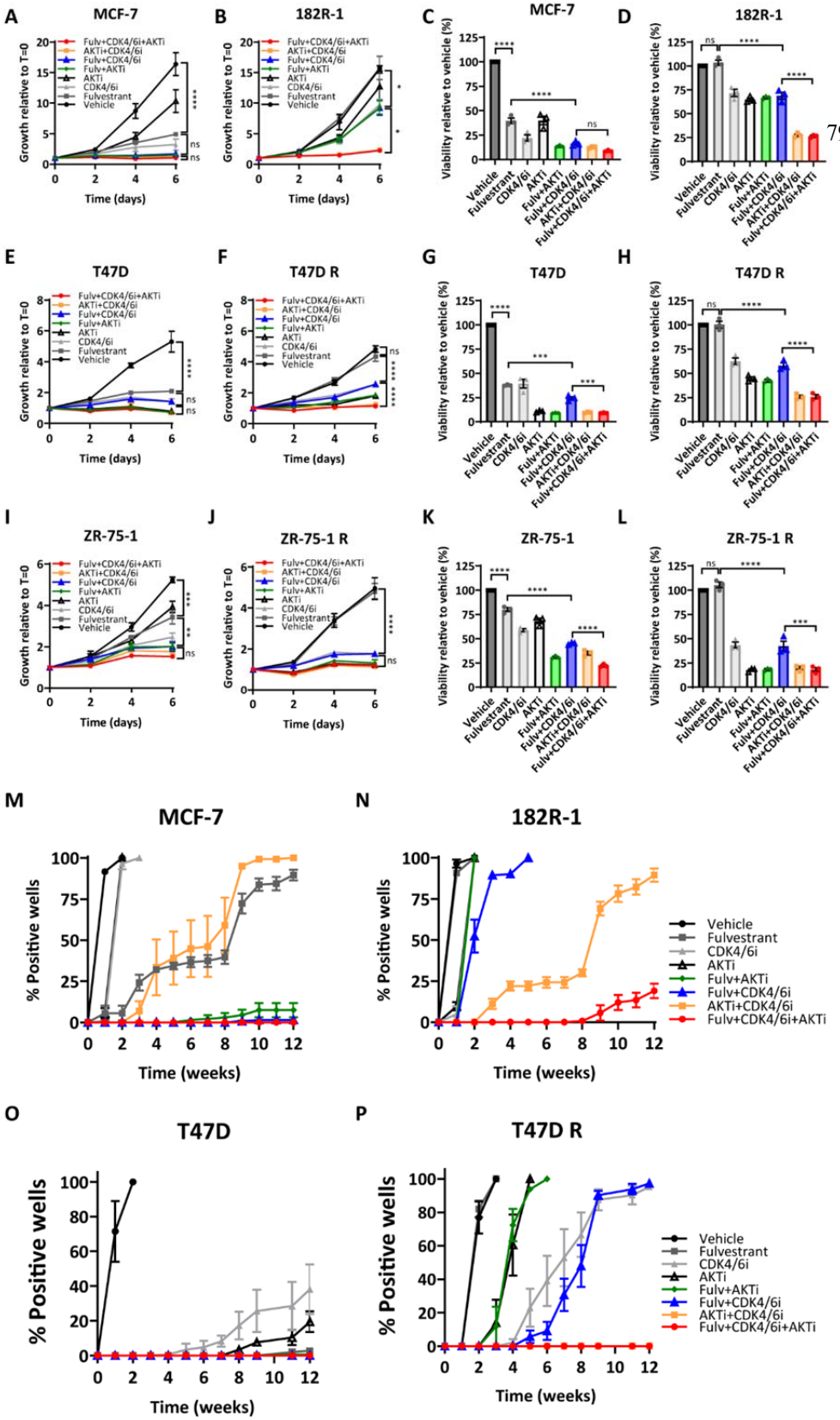

Fig. 1.

Combined fulvestrant, CDK4/6i and AKTi is required to significantly and durably inhibit growth in ER+ fulvestrant-resistant breast cancer cell lines. The effect of fulvestrant (100 nM), CDK4/6i (palbociclib, 200 nM in the MCF-7 and T47D cell models; 5 μM in the ZR-75-1 cell model) and AKTi (capivasertib, 500 nM in the MCF-7 cell model; 200 nM in the T47D model; 150 nM in the ZR-75-1 cell model), as single agents or in double and triple combinations, was assessed in all cell lines by crystal violet growth assay (**A**, **B**, **E**, **F**, **I** and **J**) and CellTiter-Blue viability assay (**C**, **D**, **G**, **H**, **K** and **L**) performed over 6 days. Outgrowth of resistant colonies was investigated in MCF-7 (**M** an **N**) and T47D models (**O** and **P**) by weekly evaluation of the percentage of 48 wells at 50% or greater confluence (positive wells) over 12 weeks. Experiments were conducted in three biological replicates and data are shown as mean ± SEM. Asterisks indicate significant differences in one-way ANOVA test at day 6 (* $0.01 < p < 0.05$, ** $0.001 < p < 0.01$, *** $0.0001 < p < 0.001$ and **** $p < 0.0001$).

Figure 2

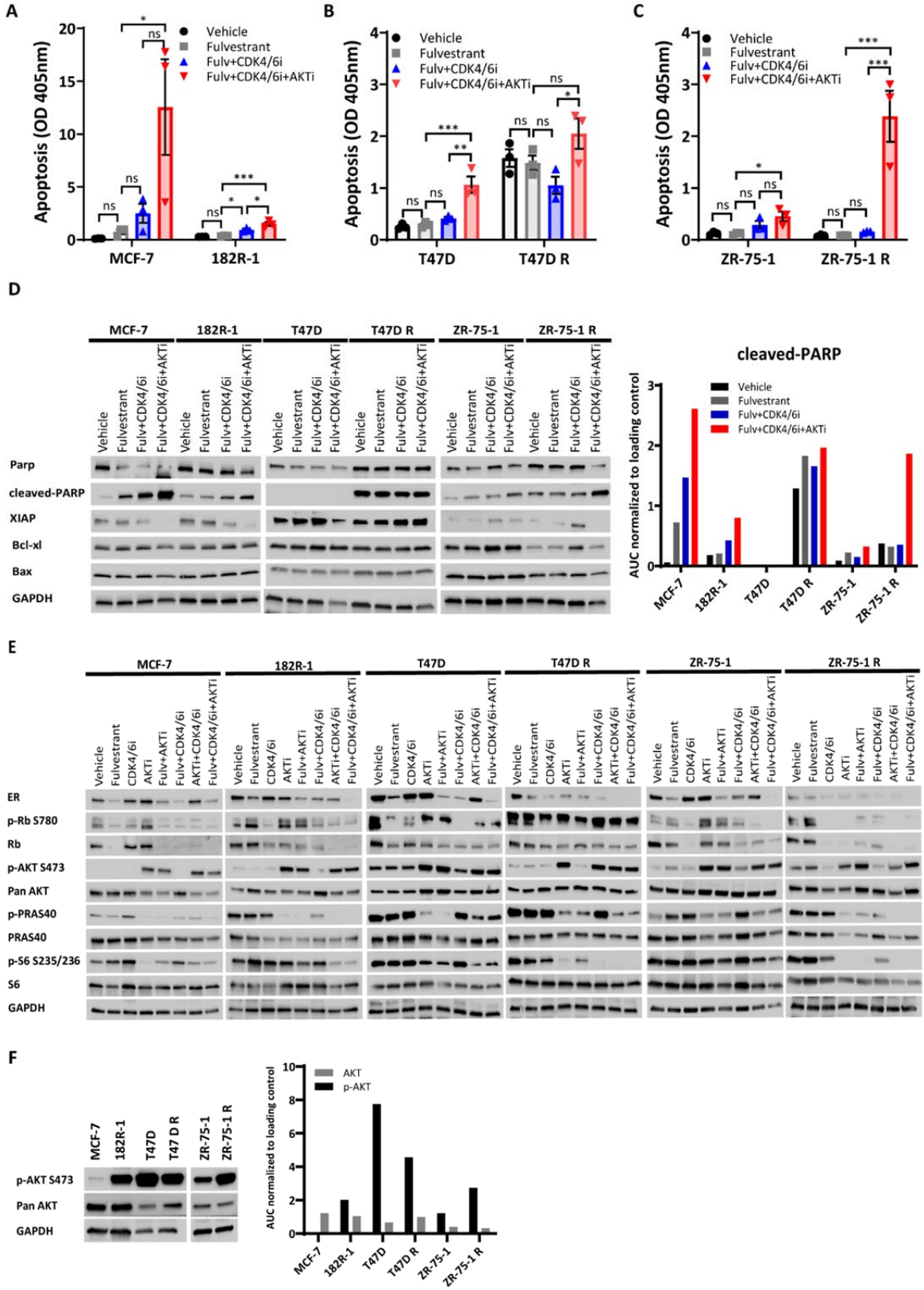
A
Apoptosis (OD 405nm)
Vehicle
Fulvestrant
Fulv+CDK4/6i
Fulv+CDK4/6i+AKTi
MCF-7
182R-1
B
T47D
T47D R
C
ZR-75-1
ZR-75-1 R
D
MCF-7
182R-1
T47D
T47D R
ZR-75-1
ZR-75-1 R
Parp
cleaved-PARP
XIAP
Bcl-xl
Bax
GAPDH
cleaved-PARP
AUC normalized to loading control
E
ER
p-Rb S780
Rb
p-AKT S473
Pan AKT
p-PRAS40
PRAS40
p-S6 S235/236
S6
F
AKT
p-AKT
AUC normalized to loading control

Fig. 2. Combined targeting of ER, CDK4/6 and AKT efficiently inhibits cyclin D/CDK4-6/Rb and PI3K/AKT-mTOR pathways in ER+ breast cancer cell lines. Apoptotic levels were determined by evaluating the presence of cytoplasmic nucleosomes in MCF-7 (**A**), T47D (**B**) and ZR-75-1 (**C**) cells using an ELISA cell death detection assay. Data are shown with error bars representing mean ± SEM of three biological replicates. Asterisks indicate significant differences in one-way ANOVA test (* $0.01 < p < 0.05$, ** $0.001 < p < 0.01$, *** $0.0001 < p < 0.001$ and **** $p < 0.0001$). (**D**) Western blot analysis of apoptosis markers in the three fulvestrant-resistant breast cancer models. Densitometry analysis of Western blot bands of cleaved-PARP was performed using ImageJ software. Data are shown as area under the curve (AUC) normalized to loading control. (**E**) Western blot analysis of key signal transduction proteins in the three fulvestrant-resistant breast cancer models. (**F**) Western blotting analysis of p-AKT (S473) and total AKT expression in the three fulvestrant-resistant breast cancer models. Densitometry analysis of Western blot bands of p-AKT (S473) and total AKT was performed using ImageJ software. Data are shown as area under the curve (AUC) normalized to loading control. GAPDH was used as loading control for Western blotting analysis. A representative of two biological replicates is shown. Both apoptosis assay and harvesting protein for Western blotting analysis were performed 3 days after treatment with fulvestrant (100 nM), CDK4/6i (palbociclib, 200 nM in the MCF-7 and T47D cell models; 5 μM in the ZR-75-1 cell model) and AKTi (capivasertib, 500 nM in the MCF-7 cell model; 200 nM in the T47D model; 150 nM in the ZR-75-1 cell model).

Figure 3

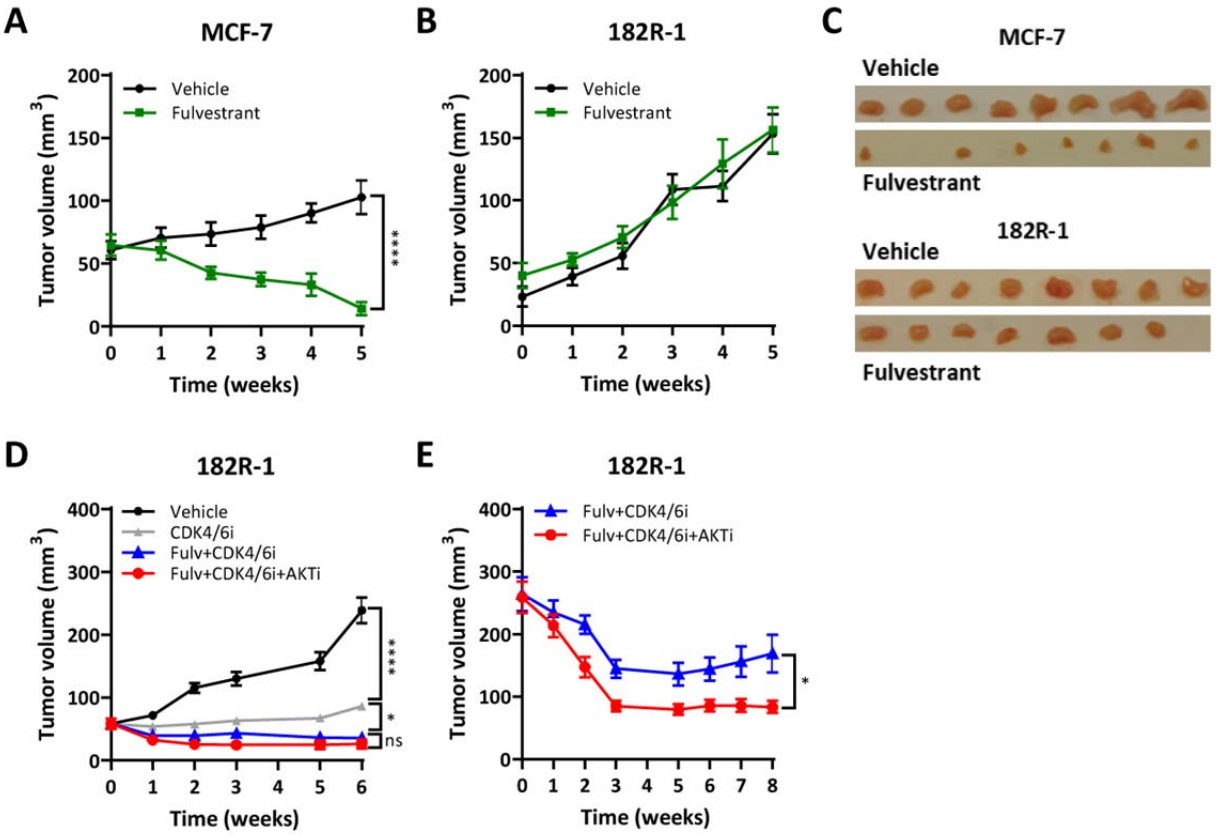

Fig. 3. Combined inhibition of CDK4/6 and AKT prevents progression in tumor xenografts resistant to fulvestrant. Tumor growth curves of MCF-7 (**A**) and 182R-1 (**B**) tumors following treatment with fulvestrant (100 mg/Kg bodyweight; N = 7) or vehicle (castor oil, N = 8) administered subcutaneously once a week. Treatment was initiated when tumors reached 50 mm^3 and continued for 5 weeks. (**C**) Mice were sacrificed on week 5 and MCF-7 and 182R-1 tumors were excised. Tumor growth curves of 182R-1 tumors treated with CDK4/6i (palbociclib, 50 mg/Kg bodyweight; N = 8) alone (**D**), in combination with fulvestrant (100mg/Kg bodyweight; N = 7 and N = 10) (**D** and **E**), or in combination with both AKTi (capivasertib 100mg/Kg bodyweight) and fulvestrant (100 mg/Kg bodyweight; N = 6 and N = 10) (**D** and **E**), or vehicle

(castor oil and 25% w/v HPB cyclodextrin; N = 8) (**D**). CDK4/6i and AKTi were administered by oral gavage once daily for 5 days a week when tumors reached 50 mm^3 (**D**) or 250 mm^3 (**E**), and treatment was continued for up to 8 weeks. Data are shown as mean tumor volume ± SEM. Asterisks indicate significant difference in ANOVA one-way test (**D**) or two-tailed t-test (**A**, **B** and **E**) at the endpoint (* $0.01 < p < 0.05$, ** $0.001 < p < 0.01$, *** $0.0001 < p < 0.001$ and **** $p < 0.0001$).

Figure 4

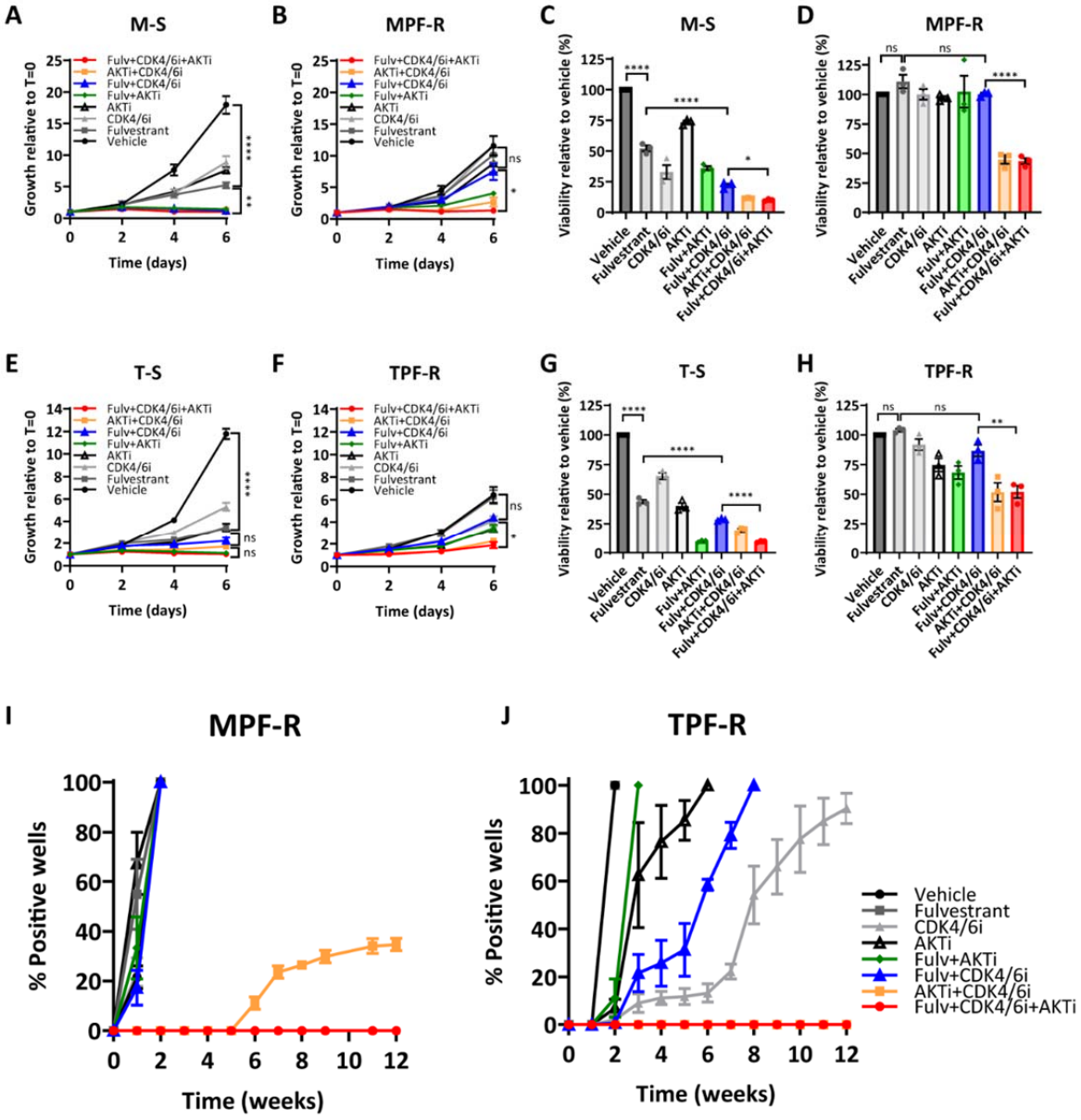

Fig. 4. Combined fulvestrant, CDK4/6i and AKTi is effective in breast cancer cell lines resistant to combined CDK4/6i and fulvestrant. The effect of fulvestrant (100 nM), CDK4/6i (palbociclib, 200 nM) and AKTi (capivasertib, 250-500 nM in the MCF-7 cell model; 100 nM in the T47D cell model), as single agents or in double and triple combination, was assessed in all cell lines by crystal violet growth assay (**A**, **B**, **E** and **F**), CellTiter-Blue viability assay (**C**, **D**, **G**

and **H**) performed over 6 days. Outgrowth of resistant colonies was investigated in MPF-R (**I**) and TPF-R (**J**) cells by weekly evaluation of the percentage of 48 wells at 50% or greater confluence (positive wells) over 12 weeks. Experiments were conducted in three biological replicates and data are shown as mean ± SEM. Asterisks indicate significant differences in one-way ANOVA tests at day 6 (* $0.01 < p < 0.05$, ** $0.001 < p < 0.01$, *** $0.0001 < p < 0.001$ and **** $p < 0.0001$).

Figure 5

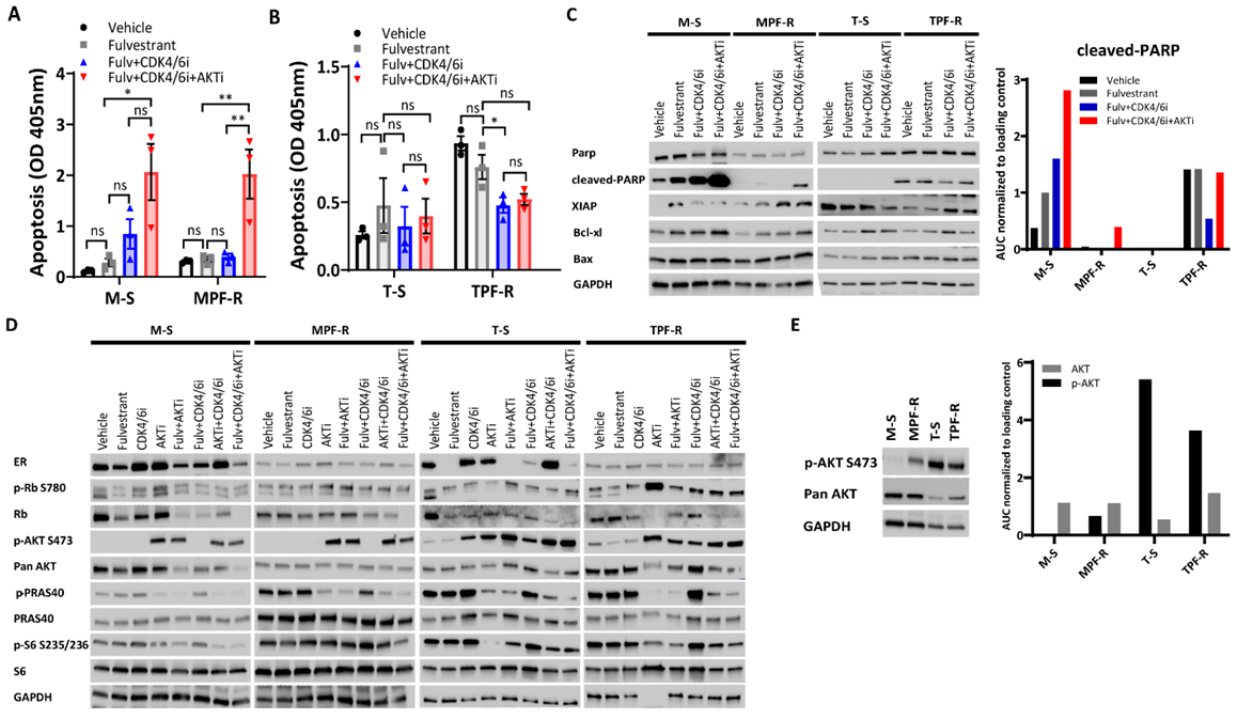

882

883 **Fig. 5. Combined targeting of ER, CDK4/6 and AKT efficiently inhibits cyclin D/CDK4-**
884 **6/Rb and PI3K/AKT-mTOR pathways in breast cancer cells resistant to combined**
885 **CDK4/6i and fulvestrant.** Apoptotic levels were determined by evaluating the presence of
886 cytoplasmic nucleosomes in MCF-7 (**A**) and T47D (**B**) cell models using an ELISA cell death
887 detection assay. Data are shown with error bars representing mean ± SEM of three biological
888 replicates. Asterisks indicate significant differences in one-way ANOVA tests (* $0.01 < p < 0.05$,
889 ** $0.001 < p < 0.01$, *** $0.0001 < p < 0.001$ and **** $p < 0.0001$). (**C**) Western blot analysis of
890 apoptosis markers in both models resistant to combined fulvestrant and CDK4/6i. Densitometry
891 analysis of Western blot bands of cleaved-PARP was performed using ImageJ software. Data are
892 shown as area under the curve (AUC) normalized to loading control. (**D**) Western blot analysis
893 of key signal transduction proteins in breast cancer cell models resistant to combined CDK4/6i
894 and fulvestrant therapy. (**E**) Western blotting analysis of p-AKT (S473) and total AKT

expression in both breast cancer models resistant to combined fulvestrant and CDK4/6i. Densitometry analysis of Western blot bands of p-AKT (S473) and total AKT was performed using ImageJ software. Data are shown as area under the curve (AUC) normalized to loading control. GAPDH was used as loading control for Western blotting analysis. A representative of two biological replicates is shown. Both apoptosis assay and harvesting protein for Western blotting analysis were performed 3 days after treatment with fulvestrant (100 nM), CDK4/6i (palbociclib, 200 nM) and AKTi (capivasertib, 250 nM in the MCF-7 cell model; 100 nM in the T47D cell model).

Figure 6

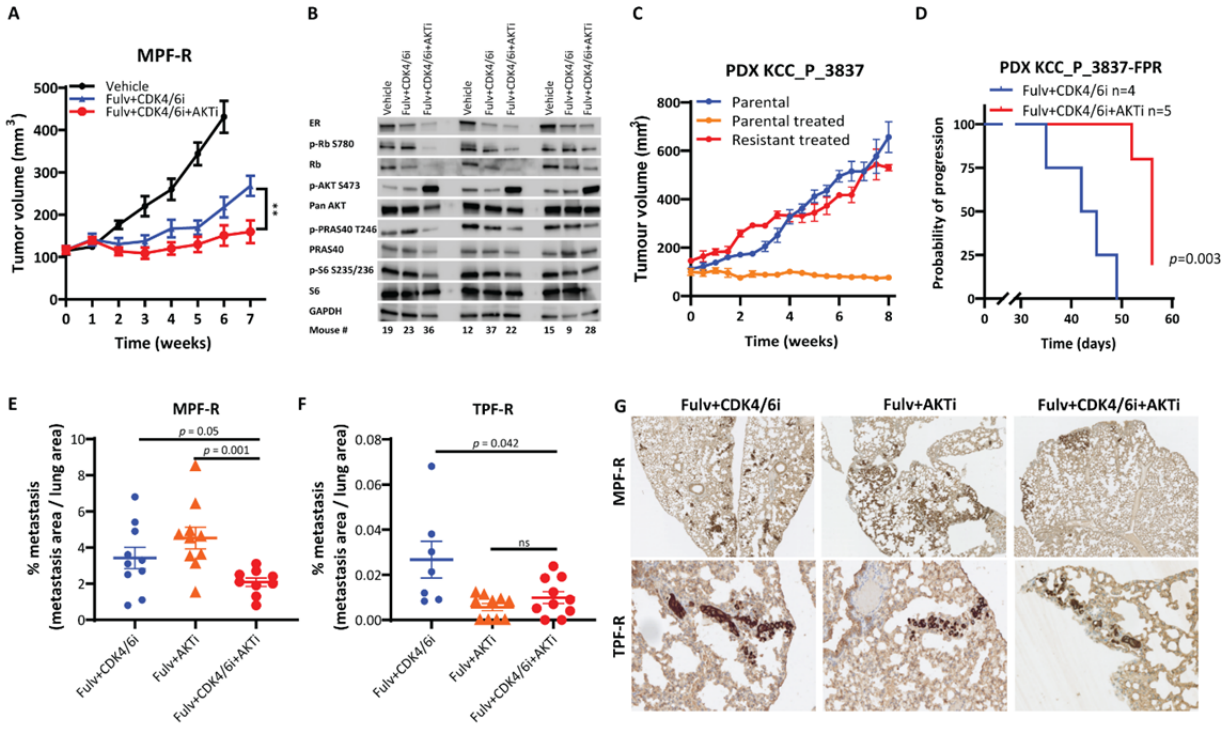

Fig. 6. Combined fulvestrant, CDK4/6i and AKTi is effective in tumor xenografts resistant to combined CDK4/6i and fulvestrant. (**A**) Tumor growth curves of orthotopic MPF-R tumors treated with CDK4/6i (palbociclib, 50 mg/Kg bodyweight) combined with fulvestrant (100mg/Kg bodyweight; N = 9) or in combination with both AKTi (capivasertib, 100 mg/Kg bodyweight) and fulvestrant (100 mg/Kg bodyweight; N = 10), or vehicle (castor oil and 25% w/v HPB cyclodextrin; N = 10). CDK4/6i and AKTi were administered by oral gavage once daily for 5 days a week, whereas fulvestrant was administered subcutaneously once a week. Treatment was initiated when tumors reached 100 mm^3 and continued for up to 7 weeks. Mice from the control group were sacrificed and tumors excised on week 6 due to their large size, while mice from double and triple combination groups were sacrificed and tumors excised on week 7. Data are shown as mean tumor volume ± SEM. Asterisks indicate significant differences in two-tailed t-test at the endpoint (* $0.01 < p < 0.05$, ** $0.001 < p < 0.01$, *** $0.0001 < p <$

930 0.001 and **** $p < 0.0001$). (**B**) Western blot analysis of key signal transduction proteins in 3
931 tumors of each treatment group excised when mice were sacrificed. GAPDH was used as loading
932 control. (**C**) Tumor volumes over time of the parental PDX KCC_P_3837 untreated (blue) and
933 treated with combined CDK4/6i palbociclib (25 mg/kg in 2.5% DMSO, 25% β-cyclodextrin, 5
934 days per week by oral gavage) and fulvestrant (100 mg/kg in castor oil, once weekly via sub-
935 cutaneous injection) (orange), and of the derivative PDX KCC_P_3837-FPR resistant to
936 combined palbociclib and fulvestrant (red) at the third passage of continuous exposure to
937 combined palbociclib and fulvestrant. (**D**) Kaplan-Meier survival plot of progression of PDX
938 KCC_P_3837-FPR (resistant to combined CDK4/6i and fulvestrant) under treatment with
939 combined CDK4/6i and fulvestrant with or without AKTi capivasertib (100 mg/kg in 2.5%
940 DMSO, 25% β-cyclodextrin, 5 days per week by oral gavage) (N = 5 and N = 4, respectively).
941 Progression was defined as tumors growing to at least 5 mm in the shortest dimension. A two-
942 sided p value ($p < 0.05$) was calculated using log-rank testing. (**E** and **F**) Evaluation of metastasis
943 area > 2500 μm^2 relative to lung area at the endpoint (6 weeks) using an experimental metastasis
944 model. MPF-R tumors were treated with fulvestrant (100 mg/Kg bodyweight) combined with
945 CDK4/6i (palbociclib, 25 mg/Kg bodyweight; N = 10), fulvestrant combined with AKTi
946 (capivasertib, 100 mg/Kg bodyweight; N = 10) or triple combination (N = 9). TPF-R tumors
947 were treated with the same dosage of fulvestrant and CDK4/6i and 50 mg/Kg bodyweight of
948 AKTi (N = 7 in fulvestrant and CDK4/6i group, N = 10 in fulvestrant and AKTi and N = 10 in
949 triple combination group). CDK4/6i and AKTi were administered by oral gavage once daily for
950 5 days a week, while fulvestrant was administered subcutaneously once a week. Treatment was
951 initiated 3 days before injection of cells in the tail-vein and continued for up to 6 weeks. Data are
952 shown as mean ± SEM. Significant differences were evaluated by Mann Whitney test. (**G**)

953 Representative micrographs of MPF-R and TPF-R tumors in mice lungs of each treatment group
954 showing cytokeratin expression by immunohistochemistry (5x and 20x magnification in MPF-R
955 and TPF-R, respectively).
956

Figure 7

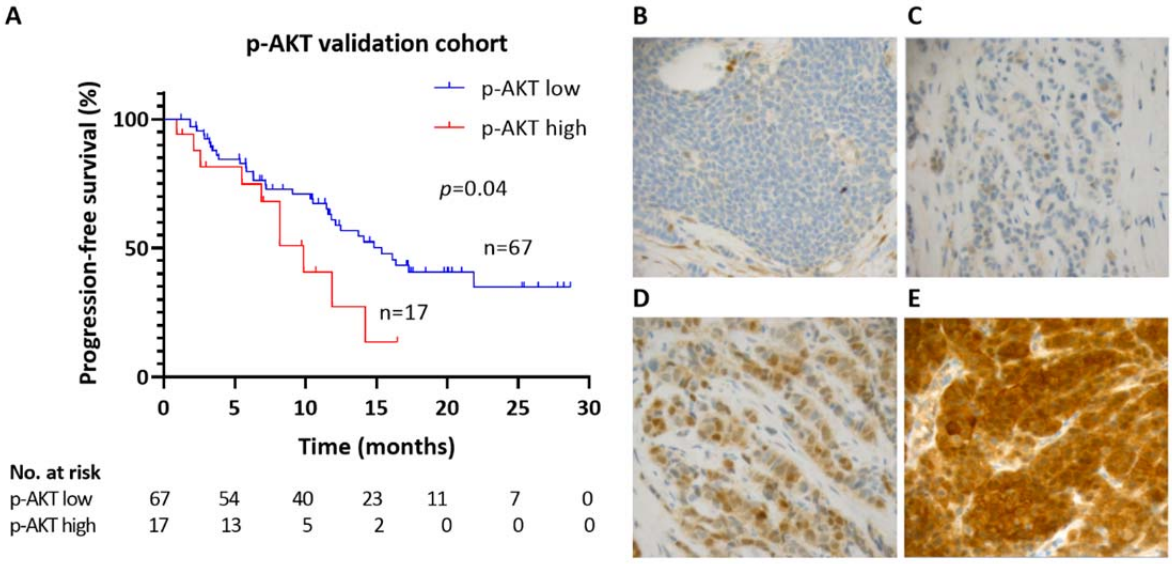

957

958 **Fig. 7. p-AKT expression correlates with PFS in ER+ metastatic breast cancer patients**
959 **treated with combined CDK4/6i and endocrine therapy.** (**A**) Kaplan-Meier plots evaluating
960 progression-free survival (PFS) according to p-AKT (S473) levels in ER+ metastatic lesions
961 from a validation cohort of ER+ breast cancer patients treated with combined CDK4/6i and
962 endocrine therapy in the advanced setting. A two-sided *p* value ($p < 0.05$) was calculated using
963 log-rank testing. Representative micrographs of breast cancer metastasis sections showing low p-
964 AKT expression (H-score < 150, **B** and **C**) or high p-AKT expression (H-score ≥ 150, **D** and **E**;
965 40x magnification).

966

Tables

Table 1. Clinical and pathological characteristics of ER+ breast cancer patients with advanced disease treated with CDK4/6i and endocrine treatment from pilot and validation cohorts according to p-AKT levels

Parameters	Pilot				Validation				Pilot vs. validation			
	p-AKT low	p-AKT high	N	p^a	p-AKT low	p-AKT high	N	p^a	pilot	validation	N	p^a
Age at starting CDK4/6i												
≤ 50	1	1	2	0.33	5	2	7	0.63	2	7	9	0.65
> 50	13	2	15		62	15	77		15	77	92	
Site of relapse [b]												
Soft tissue	9	1	10		20	5	25		10	25	35	
Bone	3	2	5	0.53	34	5	39	0.13	5	39	44	0.37
Viscera	2	0	2		13	7	20		2	20	22	
No metastatic sites												
1	4	1	5		18	6	24		5	24	29	
2	7	1	8	0.86	19	3	22	0.62	8	22	30	0.16
≥ 3	3	1	4		30	8	38		4	38	42	
Chemotherapy [c]												
No	9	1	10	0.54	37	8	45	0.60	10	45	55	0.79
Yes	5	2	7		30	9	39		7	39	46	
Time to recurrence (years)												
≤ 5	7	3	10		28	5	33		10	33	43	
1-10	4	0	4	0.28	16	7	23	0.35	4	23	27	0.29
> 10	3	0	3		23	5	28		3	28	31	
Total	14	3	17		67	17	84		17	84	101	

[a] $\chi 2$ or Fisher's exact test

[b] Site of relapse of the metastatic lesion used to evaluate p-AKT expression

[c] Includes chemotherapy administrated in the adjuvant and metastatic settings

Figure 1

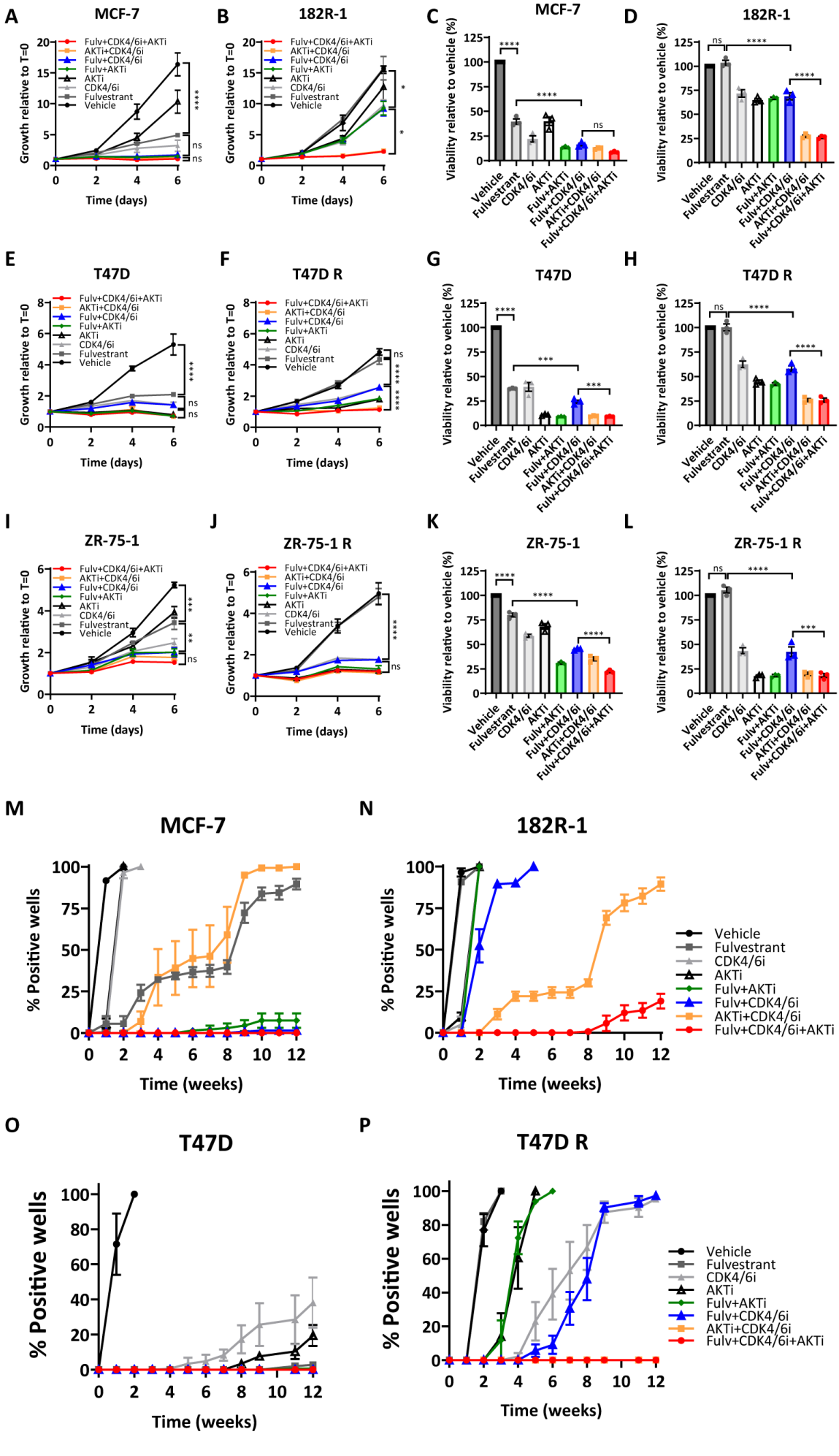
A
MCF-7
B
182R-1
C
MCF-7
D
182R-1
E
T47D
F
T47D R
G
T47D
H
T47D R
I
ZR-75-1
J
ZR-75-1 R
K
ZR-75-1
L
ZR-75-1 R
Fulv+CDK4/6i+AKTi
AKTi+CDK4/6i
Fulv+CDK4/6i
Fulv+AKTi
AKTi
CDK4/6i
Fulvestrant
Vehicle
Growth relative to T=0
Time (days)
Viability relative to vehicle (%)
ns
M
MCF-7
N
182R-1
O
T47D
P
T47D R
% Positive wells
Time (weeks)

Figure 2

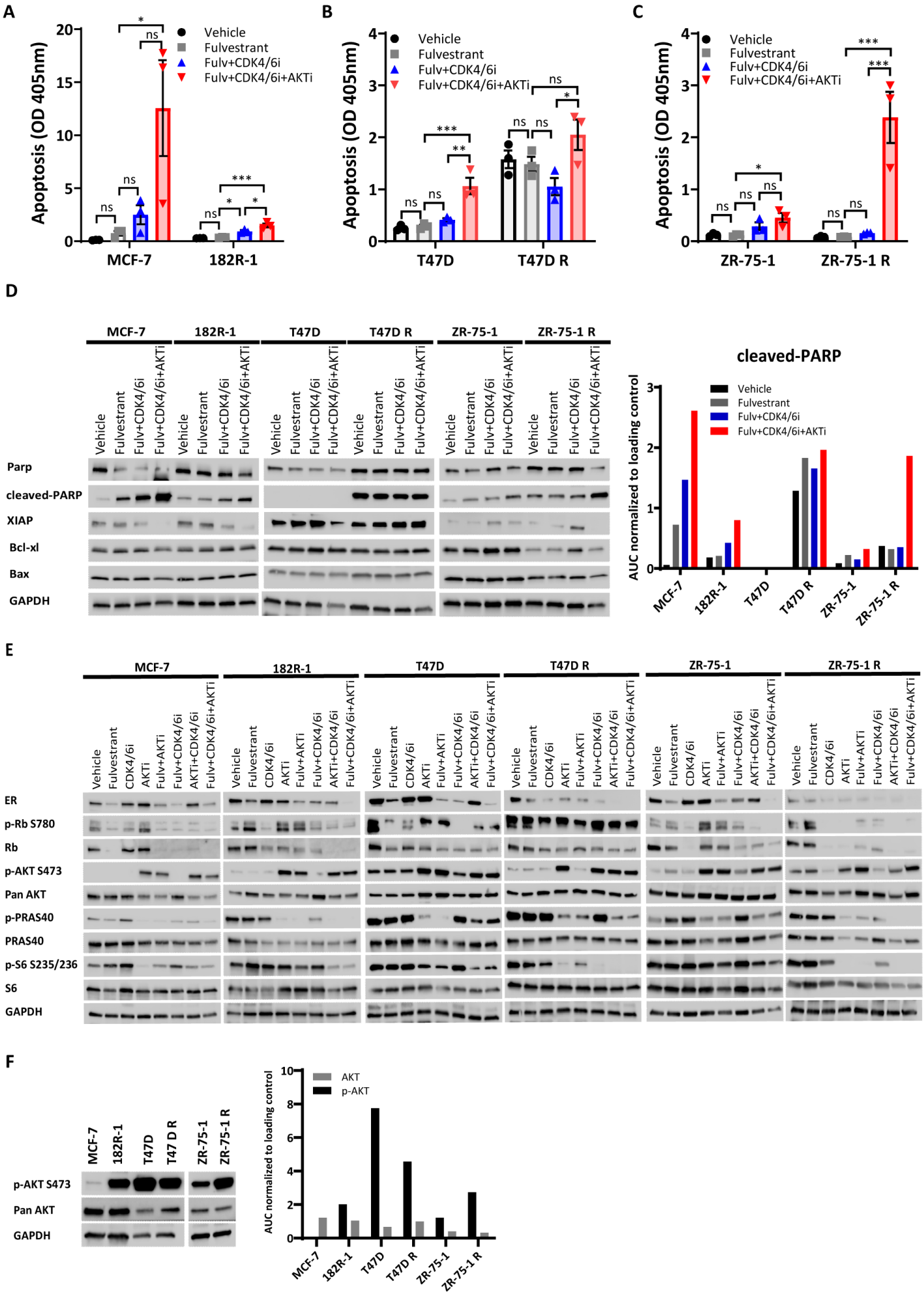
A
Apoptosis (OD 405nm)
Vehicle
Fulvestrant
Fulv+CDK4/6i
Fulv+CDK4/6i+AKTi
MCF-7
182R-1
B
T47D
T47D R
C
ZR-75-1
ZR-75-1 R
D
MCF-7
182R-1
T47D
T47D R
ZR-75-1
ZR-75-1 R
Parp
cleaved-PARP
XIAP
Bcl-xl
Bax
GAPDH
cleaved-PARP
AUC normalized to loading control
E
ER
p-Rb S780
Rb
p-AKT S473
Pan AKT
p-PRAS40
PRAS40
p-S6 S235/236
S6
F
AKT
p-AKT

Figure 3

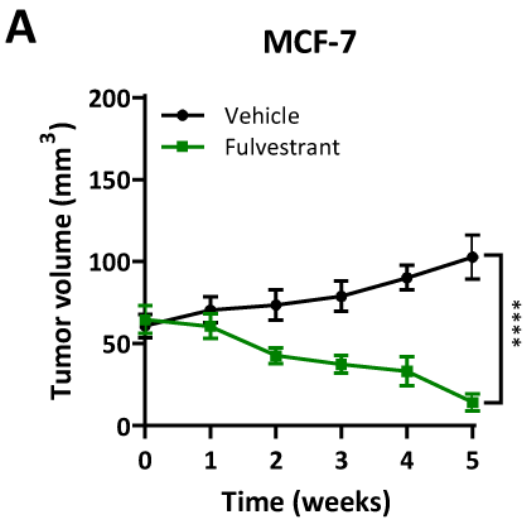
A
MCF-7
Vehicle
Fulvestrant
Tumor volume (mm3)
Time (weeks)
****

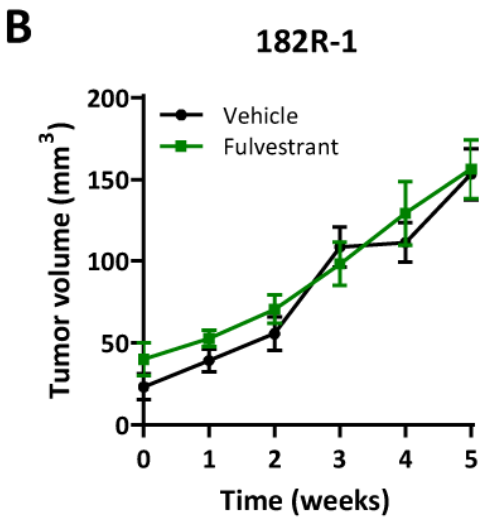
B
182R-1
Vehicle
Fulvestrant
Tumor volume (mm3)
Time (weeks)

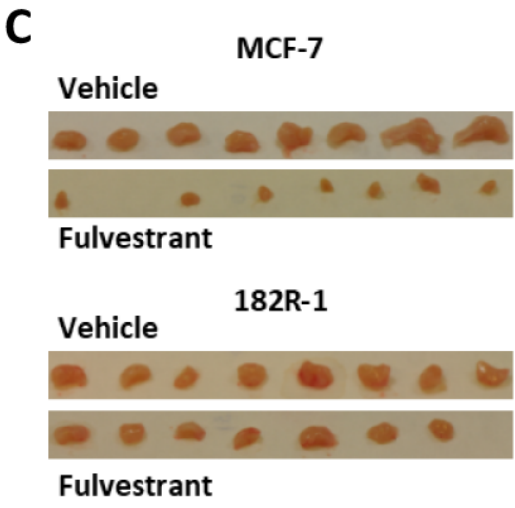
C
MCF-7
Vehicle
Fulvestrant
182R-1
Vehicle
Fulvestrant

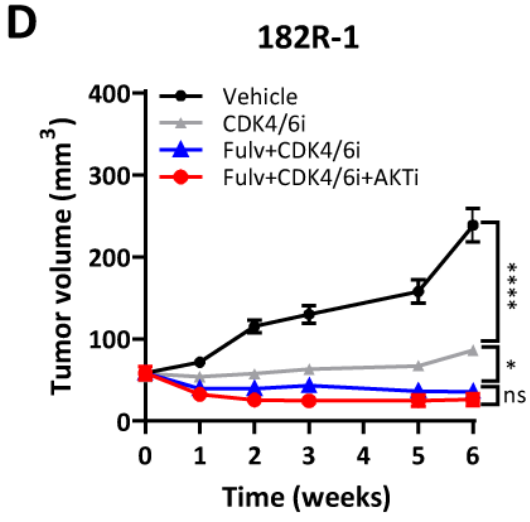
D
182R-1
Vehicle
CDK4/6i
Fulv+CDK4/6i
Fulv+CDK4/6i+AKTi
Tumor volume (mm3)
Time (weeks)
****
*
ns

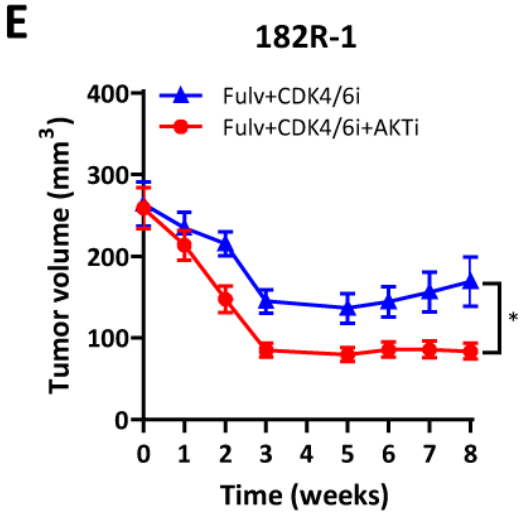
E
182R-1
Fulv+CDK4/6i
Fulv+CDK4/6i+AKTi
Tumor volume (mm3)
Time (weeks)
*

Figure 4

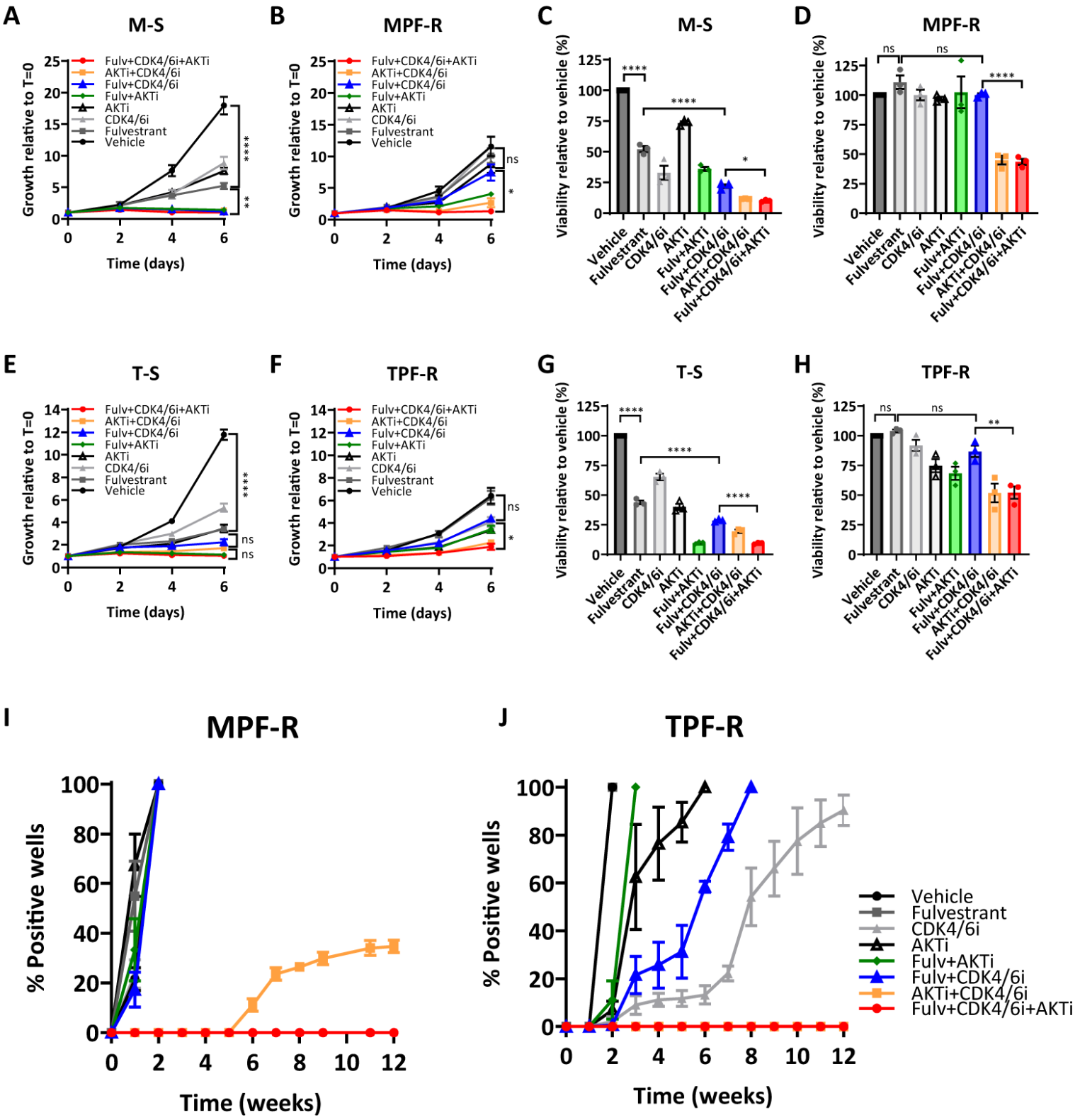
A
M-S
B
MPF-R
C
M-S
D
MPF-R
E
T-S
F
TPF-R
G
T-S
H
TPF-R
I
MPF-R
J
TPF-R
Growth relative to T=0
Time (days)
Viability relative to vehicle (%)
% Positive wells
Time (weeks)
Vehicle
Fulvestrant
CDK4/6i
AKTi
Fulv+AKTi
Fulv+CDK4/6i
AKTi+CDK4/6i
Fulv+CDK4/6i+AKTi
ns
****
**
*

Figure 5

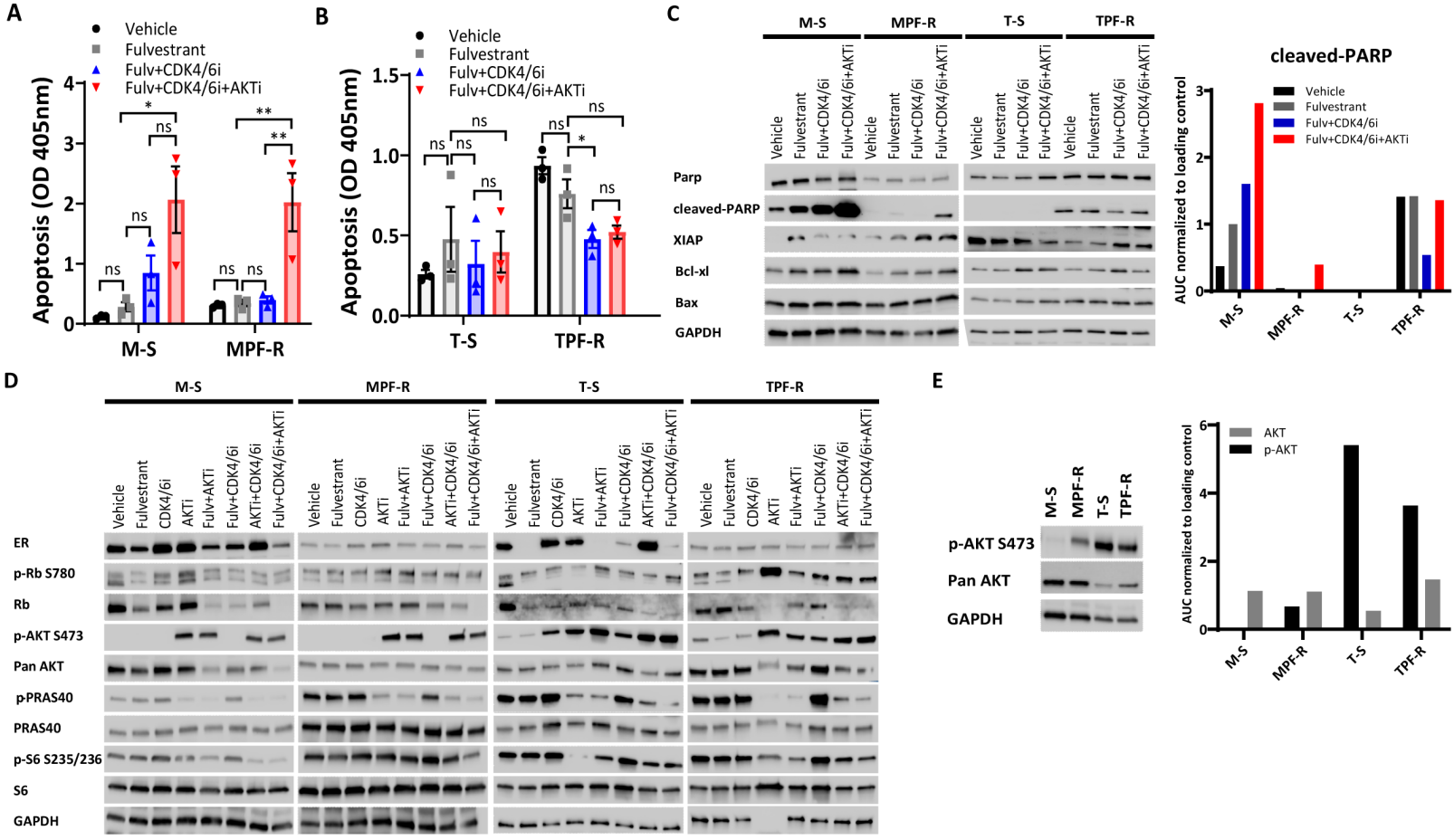
A
Vehicle
Fulvestrant
Fulv+CDK4/6i
Fulv+CDK4/6i+AKTi
Apoptosis (OD 405nm)
M-S
MPF-R
B
Apoptosis (OD 405nm)
T-S
TPF-R
C
M-S
MPF-R
T-S
TPF-R
Parp
cleaved-PARP
XIAP
Bcl-xl
Bax
GAPDH
cleaved-PARP
AUC normalized to loading control
D
ER
p-Rb S780
Rb
p-AKT S473
Pan AKT
p-PRAS40
PRAS40
p-S6 S235/236
S6
GAPDH
E
p-AKT S473
Pan AKT
GAPDH
AKT
p-AKT
AUC normalized to loading control

Figure 6

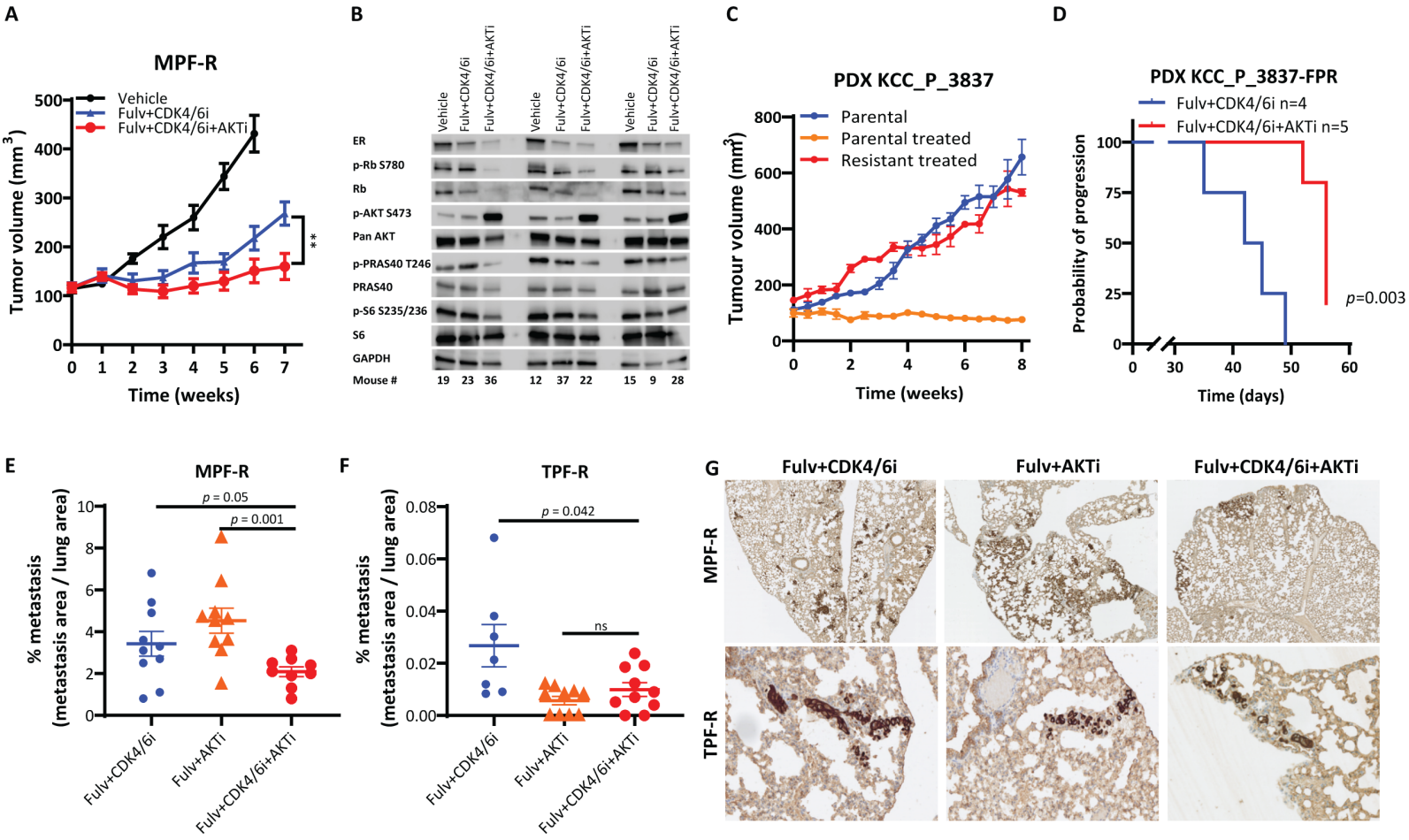
A
MPF-R
Vehicle
Fulv+CDK4/6i
Fulv+CDK4/6i+AKTi
Tumor volume (mm3)
Time (weeks)
**
B
Vehicle
Fulv+CDK4/6i
Fulv+CDK4/6i+AKTi
ER
p-Rb S780
Rb
p-AKT S473
Pan AKT
p-PRAS40 T246
PRAS40
p-S6 S235/236
S6
GAPDH
Mouse #
19 23 36 12 37 22 15 9 28
C
PDX KCC_P_3837
Parental
Parental treated
Resistant treated
Tumour volume (mm3)
Time (weeks)
D
PDX KCC_P_3837-FPR
Fulv+CDK4/6i n=4
Fulv+CDK4/6i+AKTi n=5
Probability of progression
p=0.003
Time (days)
E
MPF-R
p = 0.05
p = 0.001
% metastasis (metastasis area / lung area)
Fulv+CDK4/6i
Fulv+AKTi
Fulv+CDK4/6i+AKTi
F
TPF-R
p = 0.042
ns
% metastasis (metastasis area / lung area)
Fulv+CDK4/6i
Fulv+AKTi
Fulv+CDK4/6i+AKTi
G
Fulv+CDK4/6i
Fulv+AKTi
Fulv+CDK4/6i+AKTi
MPF-R
TPF-R

Figure 7

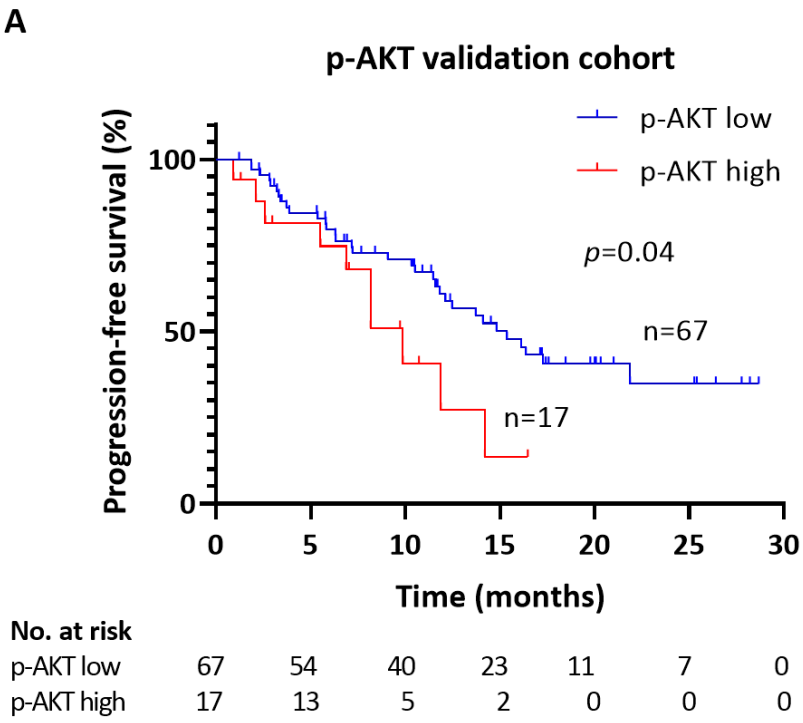
A
p-AKT validation cohort
p-AKT low
p-AKT high
p=0.04
n=67
n=17
Progression-free survival (%)
100
50
0
0
5
10
15
20
25
30
Time (months)
No. at risk
p-AKT low 67 54 40 23 11 7 0
p-AKT high 17 13 5 2 0 0 0

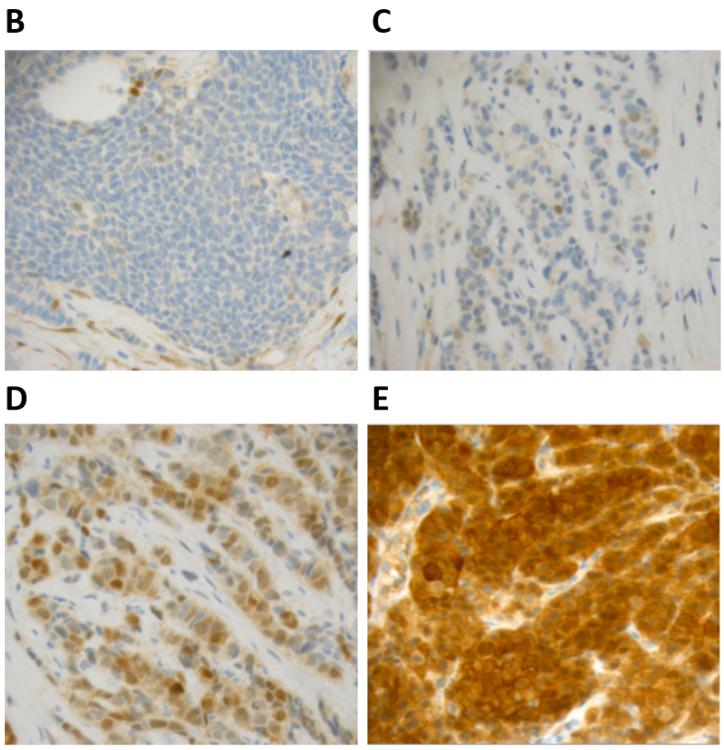
B
C
D
E